Electronic Supplementary Material (ESI) for Journal of Materials Chemistry A.

Electronic Supplementary Information

Hollow Nanoporous Covalent Triazine Frameworks via Acid Vapor-Assisted Solid Phase Synthesis for Enhanced Visible Light Photoactivity

Wei Huang, Zi Jun Wang, Beatriz Chiyin Ma, Saman Ghasimi, Dominik Gehrig, Frédéric Laquai, Katharina Landfester and Kai A. I. Zhang*

Max Planck Institute for Polymer Research, Ackermannweg 10, 55128 Mainz, Germany

Materials: 1,4-diacynobenzene (DCB), Copper cyanide, 4-bromobenzonitrile, Pd(0)$(P(Ph)_3)_4$, tetraethylorthosilicate (TEOS) and trifluromethanesulfonic acid (TfOH) were purchased from Sigma-Aldich. 4,7-bis(4,4,5,5-tetramethyl-1,3,2-dioxaborolan-2-yl)benzothiadiazole was bought from Combi-Blocks, All chemicals and solvents were used without further purification.

Characterization: UV/Vis absorption was recorded at room temperature on a Perkin Elmer Lambda 100 spectrophotometer. ^{1}H NMR measurements were recorded on Bruker Bruker AVANCE 300 system. FT-IR sepctra were recorded on a Varian 1000 FT-IR spectrometer. Solid State ^{13}C CP MAS NMR measurements were carried out using Bruker Avance II solid state NMR spectrometer operating at 300 MHz Larmor frequency equipped with a standard 4mm magic angle spinning (MAS) double resonance probe head. Scanning electron microscope (SEM) images were acquired on a LEO Gemini 1530 (Carl Zeiss AG), using an in lens SE detector. Transmission electron microscope (TEM) images were performed on a Zeiss EM912. Electron paramagnetic resonance (EPR) was measured on a Magnettech Miniscope MS200 spectrometer at room temperature. The thermal gravity analysis (TGA) measurement was conducted under oxygen with temperature increasing from 25 to 900 ^{o}C at a rate of 10 ^{o}C/min. BET surface areas and pore size distributions were measured by nitrogen adsorption and desorption at 77 K using Autosorb 1 (Quantachrome Instruments). Samples were degassed at 150 ^{o}C for 24 h under high vacuum before analysis. The BET surface area calculation was based on data points obtained from $0.02<P/P_0<0.21$ and the nonlinear density functional theory (NLDFT) equilibrium model was used for the BET model fitting. Pore size distributions and pore volumes were derived from the adsorption branches of the isotherms using Quenched Solid

Density Functional Theory (QSDFT, N_2, assuming carbon adsorbent with slit pores). X-ray diffraction (XRD) was conducted on a Philips PW 1820 diffractometer with monochromatic Cu Kα radiation. Cyclic voltammetry (CV) measurement was performed using an Autolab PGSTAT204 potentiostat/galvanostat (Metrohm). Glassy carbon electrode drop-casted with the polymers as the working electrode, Pt wire as the counter electrode, Hg/HgCl (in saturated KCl solution) electrode as the reference electrode, Bu_4NPF_6 (0.1 M in acetonitrile) was used as electrolyte. Scan rate: 100 mV/s. Time-resolved photoluminescence: Emission spectra were measured with a Streak Camera System (Hamamatsu C4742, C5680) on a nanosecond timescale. The excitation wavelength was 450 nm with ~6 ps pulse duration, using the output of an ultrafast fiber laser (Fianium SC-400-2-PP).

Monomer synthesis: 4,4'-(benzothiadiazole-4,7-diyl)dibenzonitrile (BT-Ph_2-CN_2).

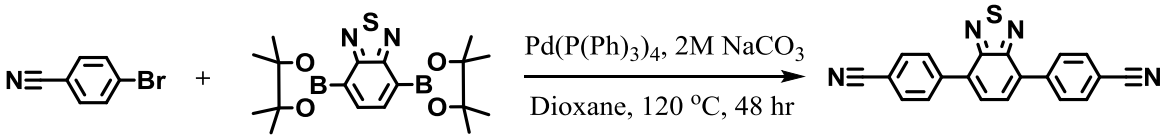

To a solution of 4,7-bis(4,4,5,5-tetramethyl-1,3,2-dioxaborolan-2-yl)benzo[c][1,2,5]thiadiazole (1.0 g, 2.6 mmol) and 4-bromobenzonitrile (1,4 g, 7.7 mmol) in 50 ml dioxane was added tetrakis(triphenylphosphine)palladium (300 mg, 260 mmol) and aqueous 2M $NaCO_3$ (20 ml), the mixture was heated at 120 ^oC under nitrogen for 24 hours. The reaction was quenched by addition of Milli Q water (30 ml). The formed solid was collected by filtration and washed thoroughly with Milli Q water, methanol and dichloromethane, respectively. The crude product was purified though silica column using dichloromethane as elute. Finally, the titled product was obtained as light yellow powder after removal of the solvent (634 mg, 72%). ^1H NMR (300 MHz, $CDCl_3$) δ 8.05 (d, 4H, ArH), δ 7.80 (d, 4H, ArH), δ 7.77 (s, 2H, ArH). ^{13}C NMR (300 MHz, $CDCl_3$) δ 153.5, 141.3, 132.6, 132.4, 129.9, 128.6, 118.7, 112.3.

Synthesis of monodispersed silica nanoparticles: The silica nanoparticles were synthesized according to Stöber method.[1] Briefly, TEOS (6 ml) was slowly added to a stirring mixture of ethanol (73.5 ml), H_2O (10 ml) and 32.8 wt% ammonia aqueous solution (3.5 ml,) with vigorous stirring. Then, the above mixture was then left stationary for 2 h at room temperature to yield uniform silica nanoparticles, the precipitated silica microspheres were separated by centrifugation and washed with ethanol, finally, dried under vacuum at 80 ^oC overnight.

Solid phase synthesis of nanoporous CTFs: nanoporous CTF-B and CTF-BT were prepared according to the same procedure. Generally, 100 mg of monomer and 300 mg silica template were well dispersed in 5 ml of tetrahydrofuran in an ultrasonic bath for 30 min. Then the solvent was removed using rotary evaporator. During this process of solvent evaporation, the silica microspheres reorganized into a 3D close-stacked structure, simultaneously, the monomer precipitated out and filled the gaps between the silica spheres to form the initial monomer/silica precursor. The formed precursor was further annealed at 80 ^{o}C for 30 min under vacuum then was carefully transferred into a small glass vial. The vial with monomer/silica precursor was placed into a conical flask, in which there was another vial with 0.3 ml TfOH. The conical flask was degassed with nitrogen and sealed followed by heated up to 100 ^{o}C in a sand bath for 24 hours. After cooled down to room temperature, the product was immersed in water and washed well with ammonia solution and Milli Q water to remove the residual TFMSA. The silica templates were etched by 20 ml of 4 M NH_4HF_2. The resultant products were washed with Milli Q water, ethanol and acetone followed by further purified with Soxlet extraction with CH_2Cl_2. After dried under vacuum at 80 ^{o}C, the products were obtained with a yield of 85-93%.

Bulk CTF-B and CTF-BT were synthesized using similar method without using silica template. Typically, 100 mg monomer and 0.3 ml TfOH are placed into a glass vial, respectively. They are then transferred into a conical flask. The flask was degassed with nitrogen and sealed before heated to desired temperature. After 24 hours, the product was washed with ammonia aqueous solution, Milli Q water and acetone followed by further purified with Soxlet extraction with CH_2Cl_2.The yield is 89 % for CTF-B and 91% for CTF-BT, respectively.

General procedure of photocatalytic reduction of 4-nitrophenol: The photocatalytic reactions were carried out in a glass vial of 20 ml at room temperature and nitrogen atmosphere. To a solution of Milli Q water (3 ml) and absolute ethanol (1 ml) was added 1 ml of 2 mM 4-NP solution, $NaBH_4$ (10 mg), 1 M NaOH (10 µl) and 5 mg of photocatalyst. The mixture was degassed with nitrogen for 5 min and stirred in the dark for 30 min. After that, the reaction vial was irradiated by a white LED light (1.2 mW/cm², λ>420 nm, OSA Opto Lights). The conversion was determined by monitoring the change in UV-Vis absorption of 4-nitrophenol.

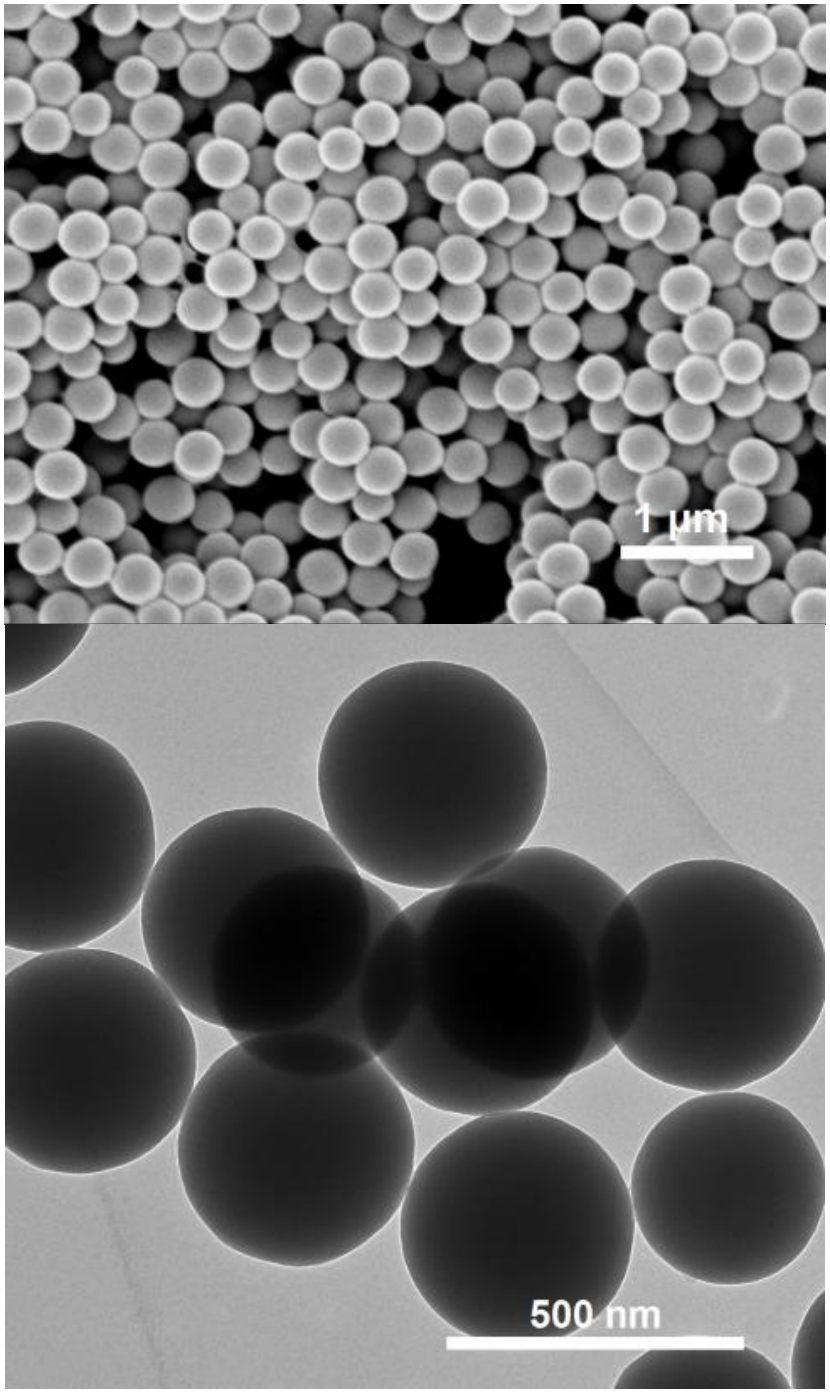

Fig. S1. SEM and TEM images of silica nanoparticles.

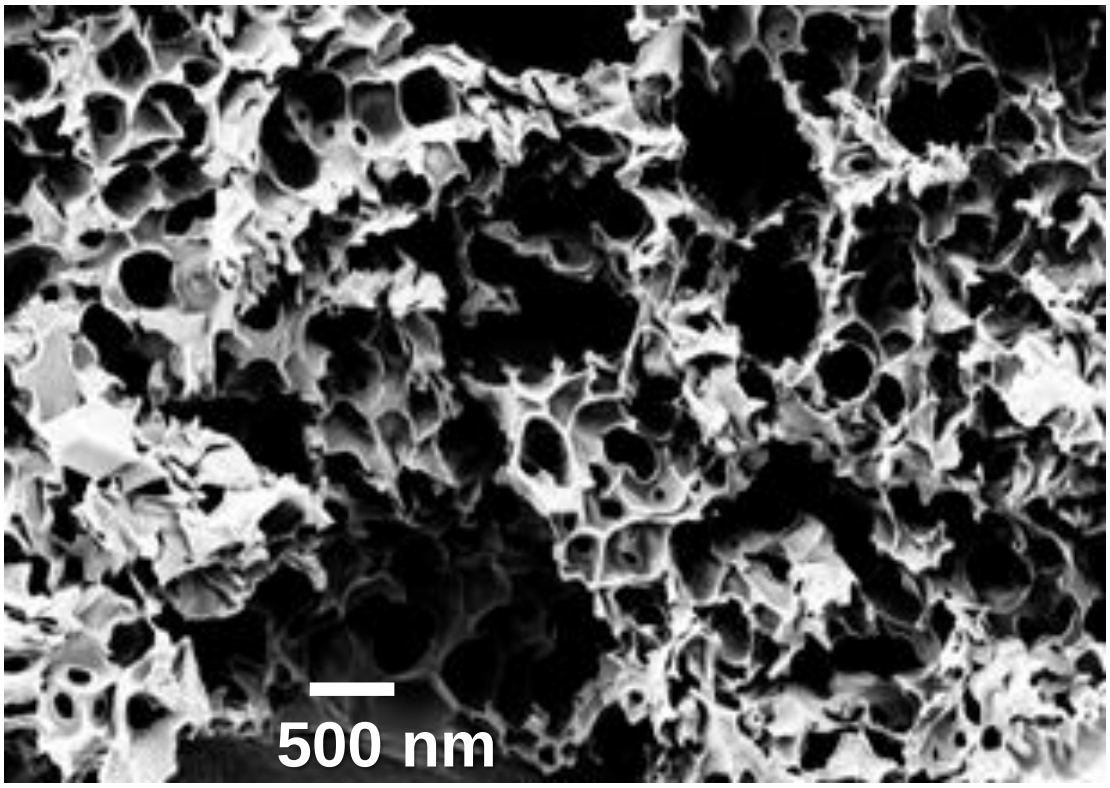

Fig. S2. SEM images of CTF-B obtained using SiO_2 nanoparticles as template in TfOH solution.

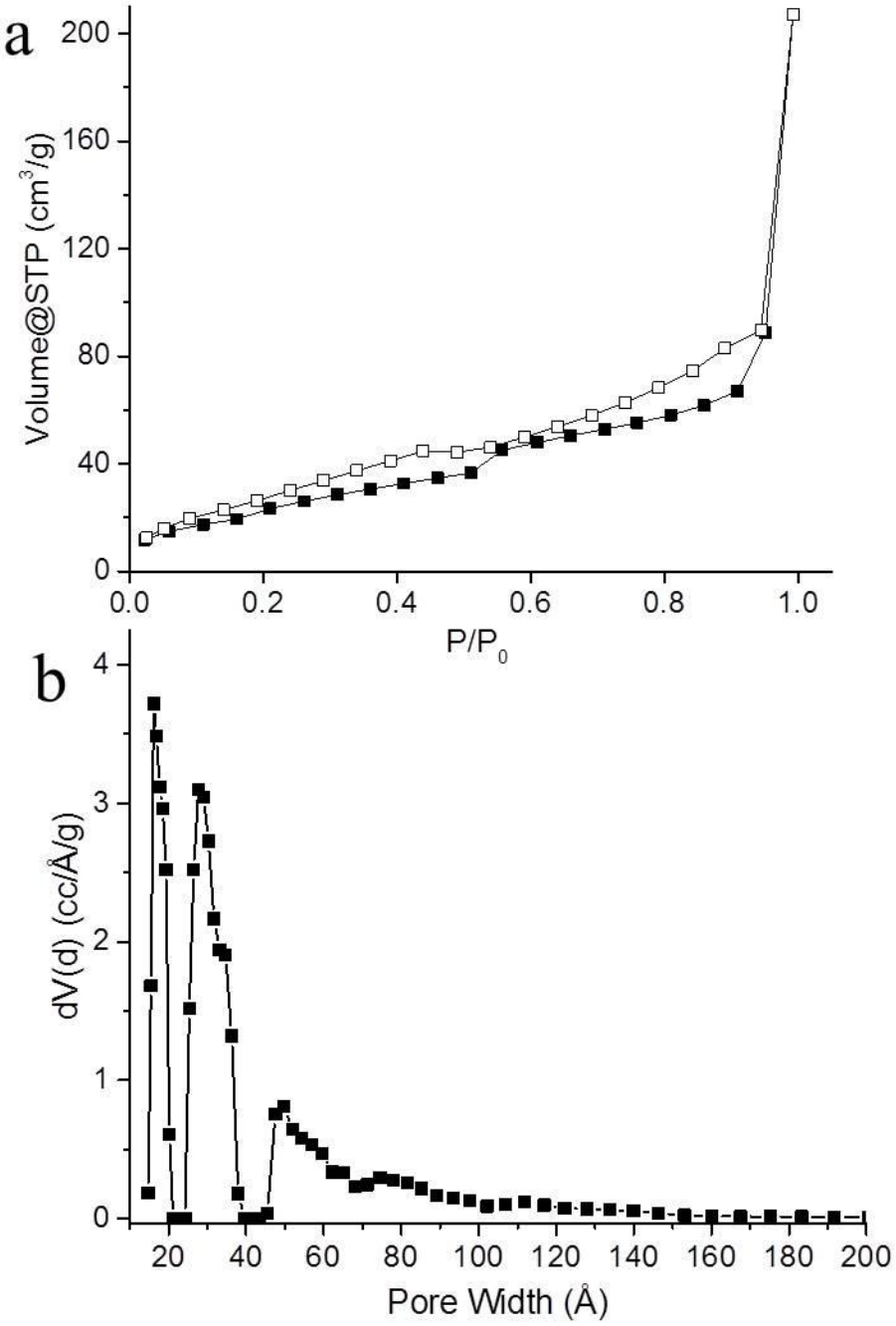

Fig. S3. (a) N_2 gas absorption-desorption isotherm of hollow CTF-BT measured at 77 K and (b) pore size distribution.

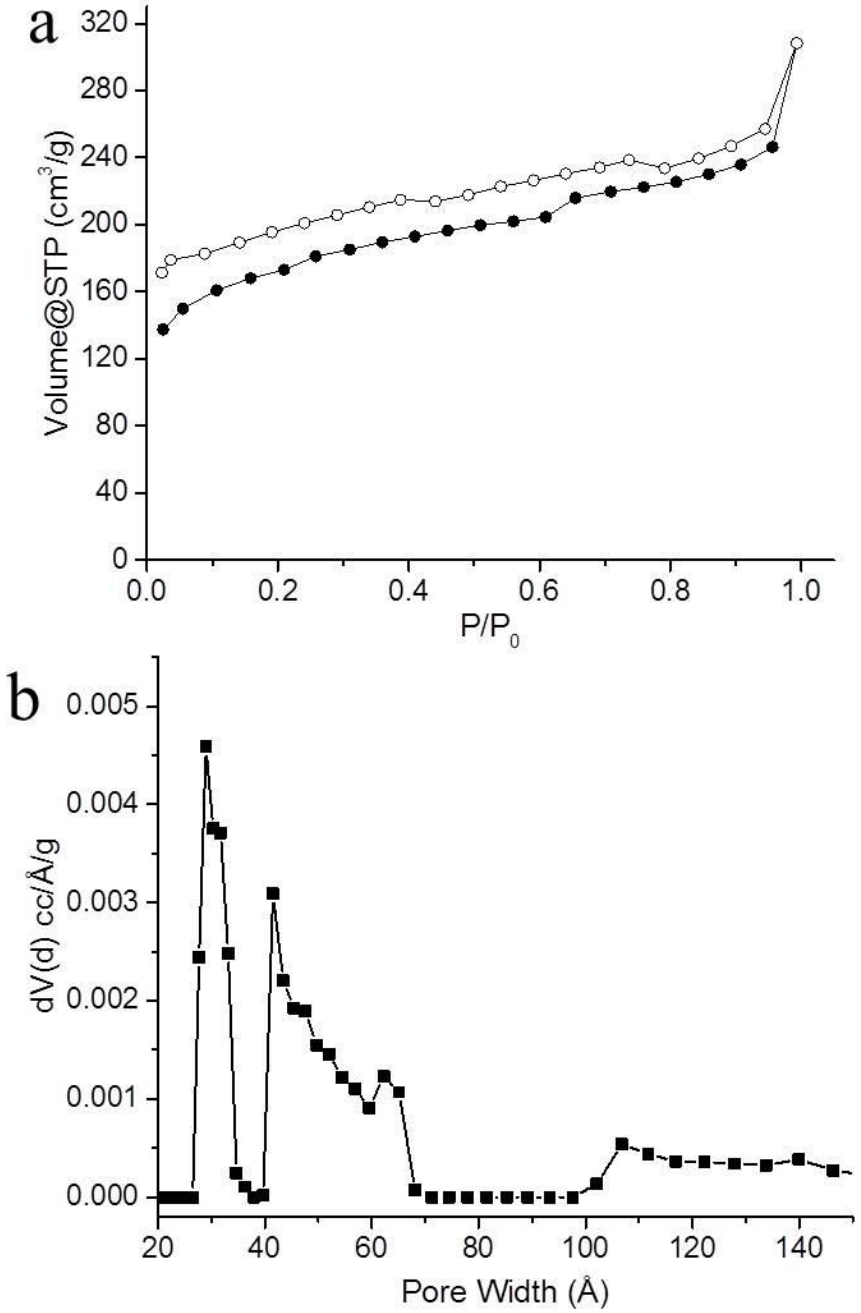

Fig. S4. (a) N_2 gas absorption-desorption isotherm of hollow CTF-B measured at 77 K and (b) pore size distribution.

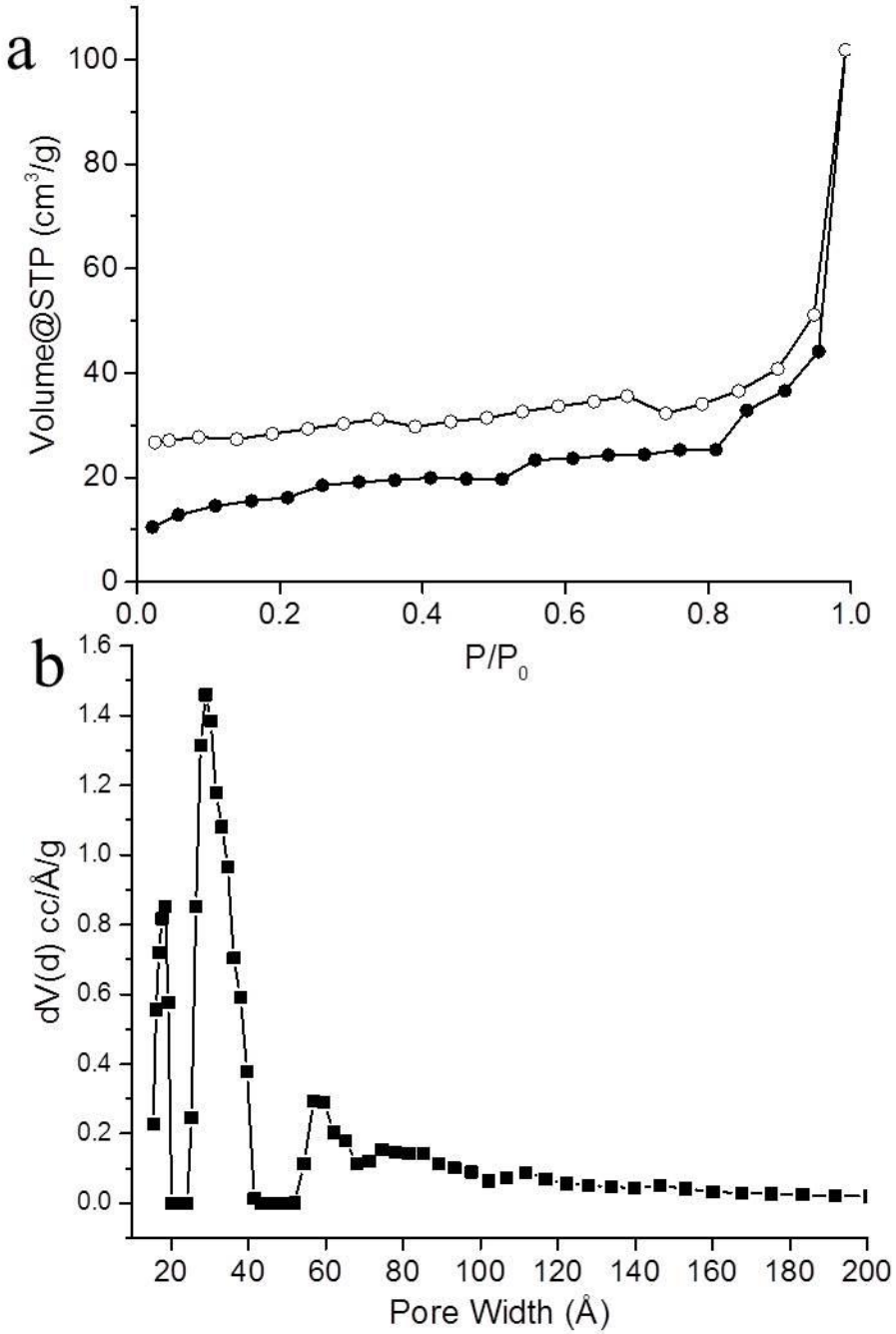

Fig. S5. (a) N_2 gas absorption-desorption isotherm of bulk CTF-BT measured at 77 K and (b) pore size distribution.

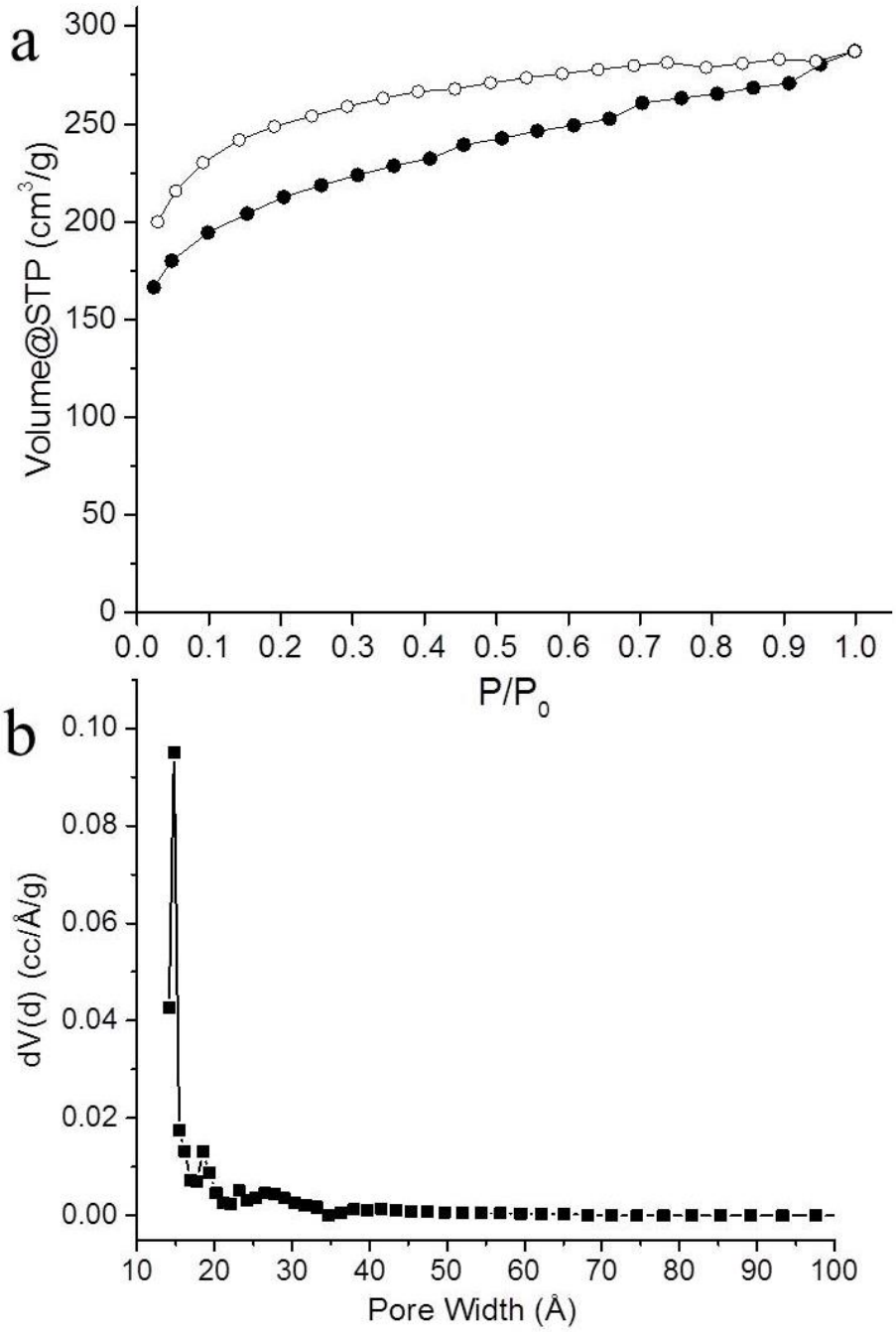

Fig. S6. (a) N_2 gas absorption-desorption isotherm of bulk CTF-B measured at 77 K and (b) pore size distribution.

Table S1. Porosity data of the CTFs.

Samples	BET surface area (m^2/g)	Pore volume (cm^3/g)	Micropore volume (cm^3/g)	Average pore size (nm)
Hollow CTF-BT	90	0.32	0.053	14.30
Bulk CTF-BT	67	0.16	0.044	9.05
Hollow CTF-B	565	0.48	0.316	3.4
Bulk CTF-B	687	0.44	0.39	2.1

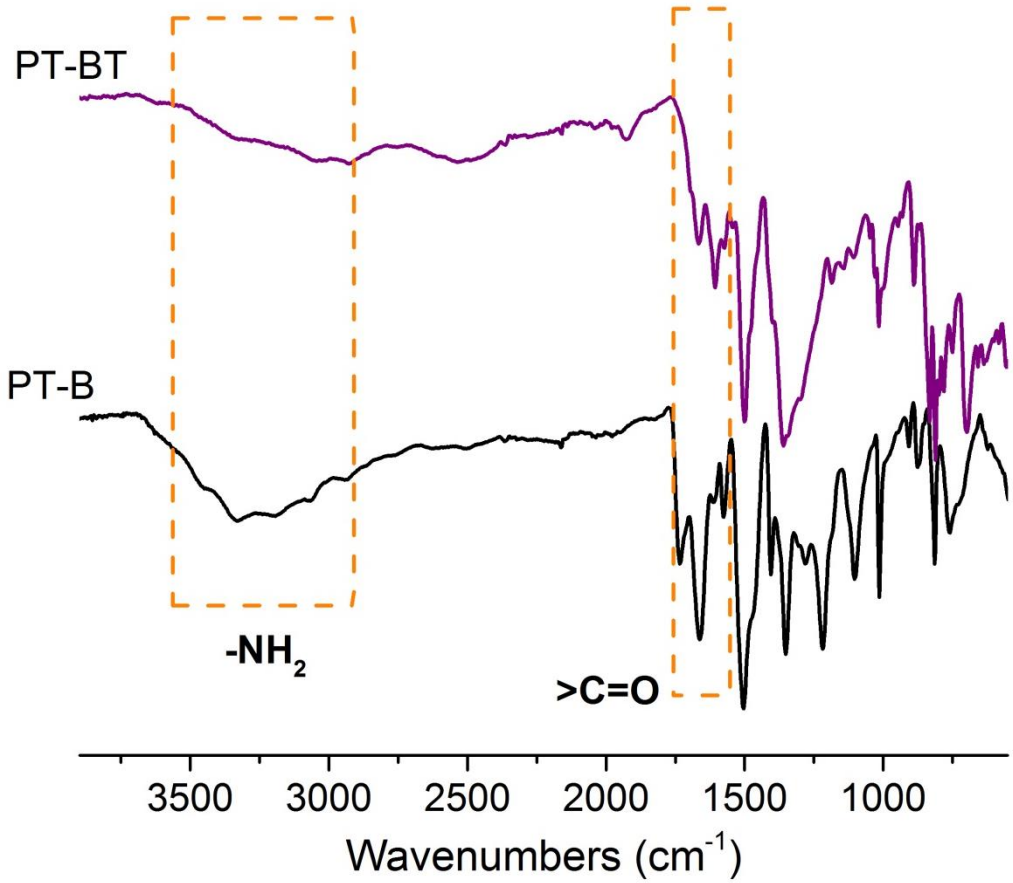

Fig. S7. FT-IR spectra of the bulk-made triazine-based polymers CTF-BT and CTF-B in TfOH solution.

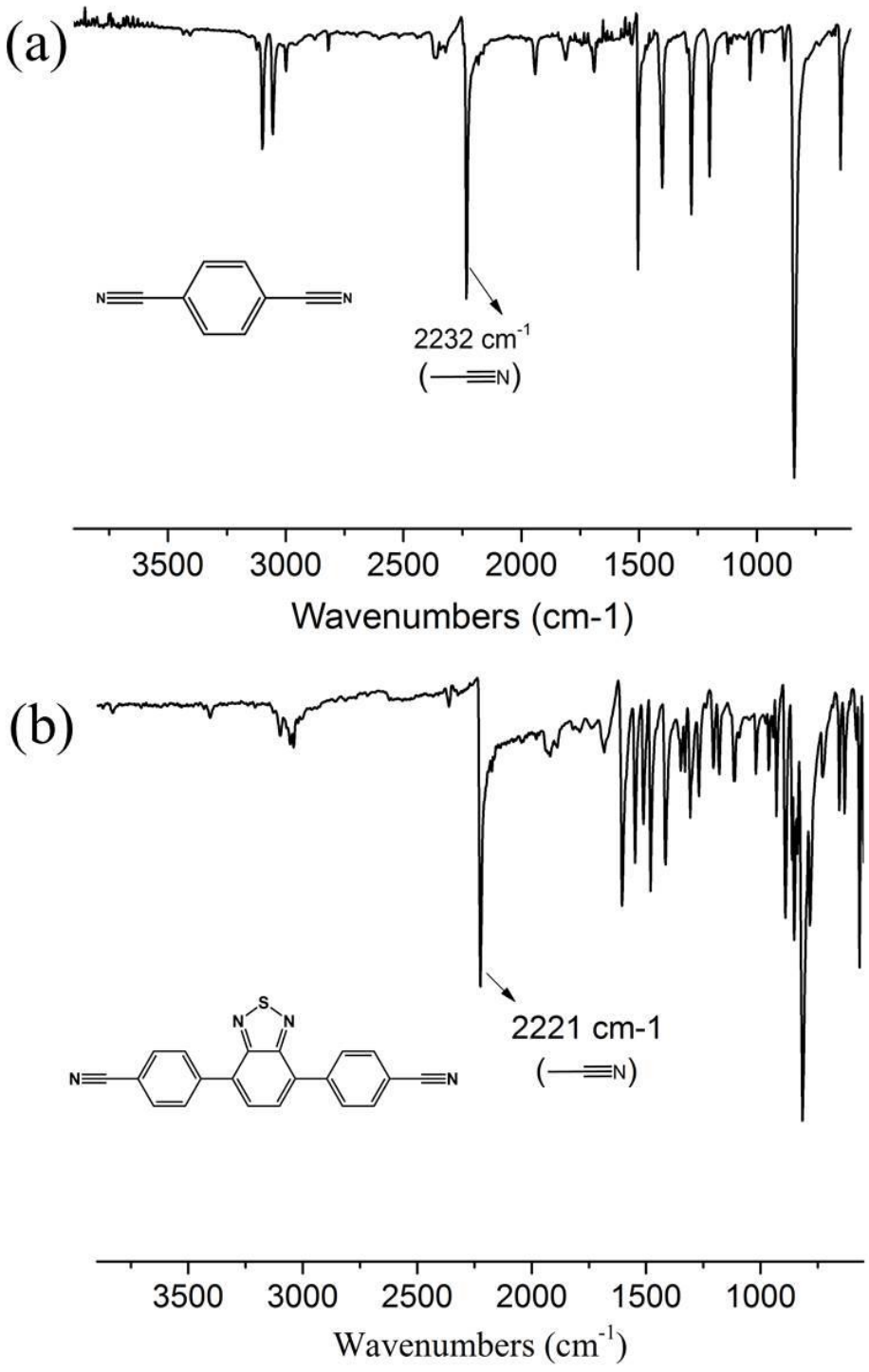

Fig. S8. FT-IR spectra of monomers: a) Ph-CN_2 and (b) BT-Ph-CN_2.

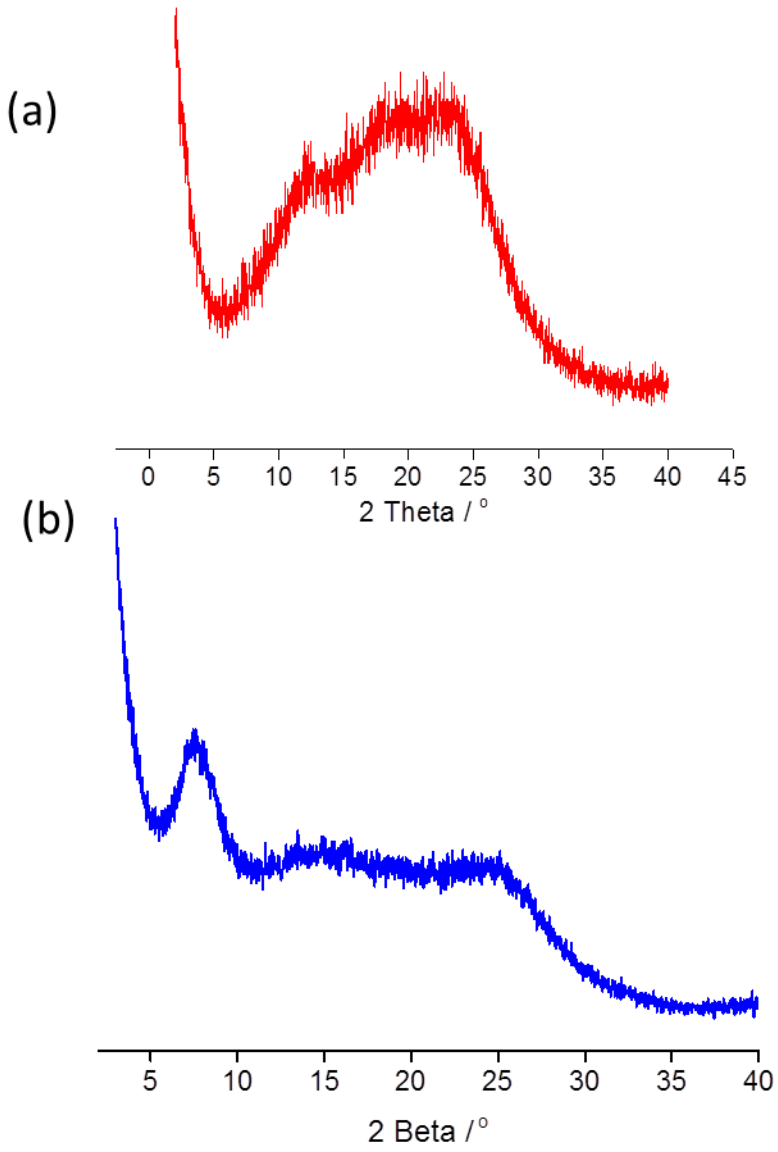

Fig. S9. Powder X-ray diffraction spectra of (a) CTF-BT and (b) CTF-B.

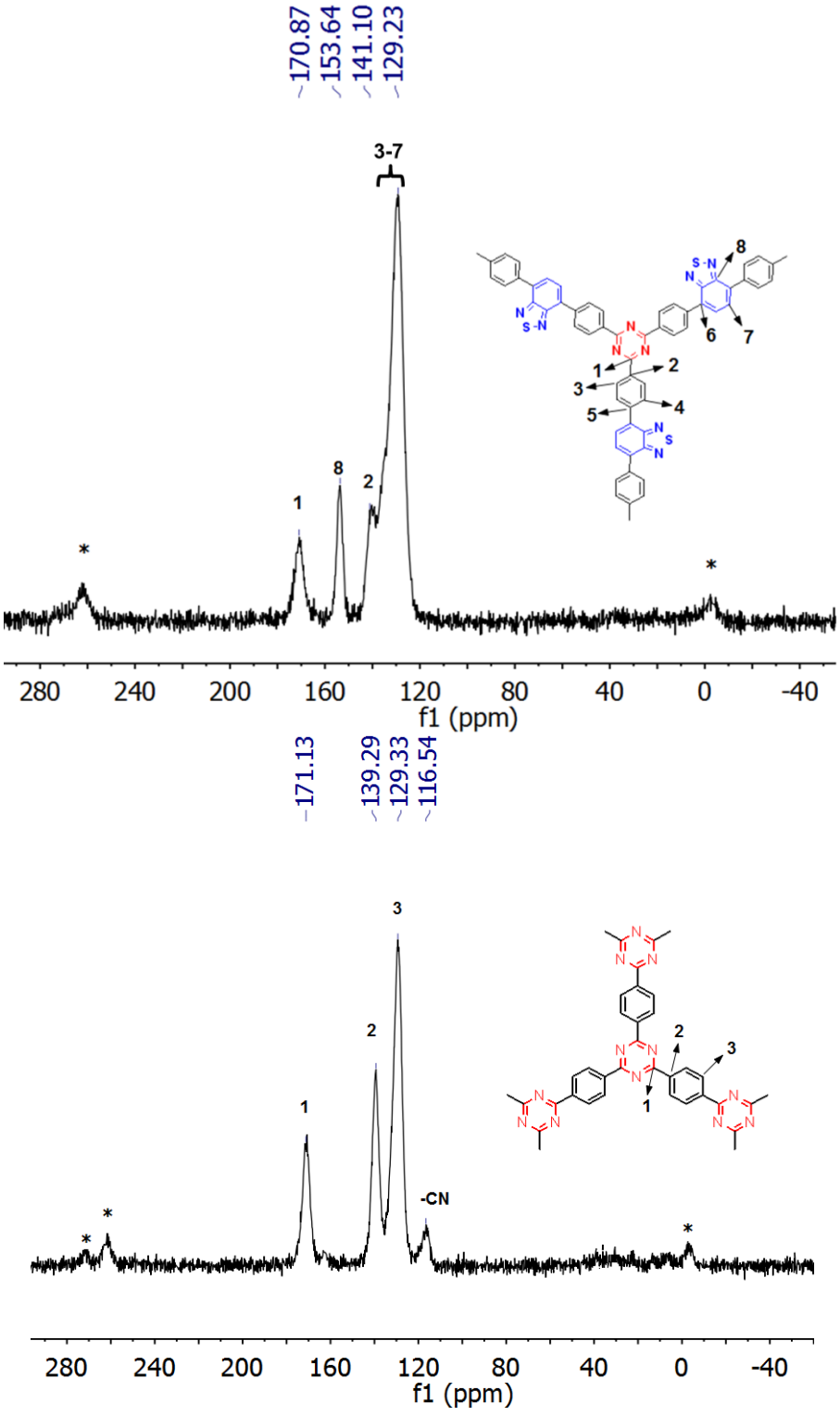

Fig. S10. Solid-state ^{13}C NMR spectra of CTF-BT and CTF-B.

Table S2. Elemental analysis data of CTF-BT and CTF-B.

Samples	Calculated (%)				Found (%)			
	C	**N**	**H**	**S**	**C**	**N**	**H**	**S**
CTF-BT	70.94	16.55	2.96	9.46	67.10	15.20	3.15	9.75
CTF-B	74.99	21.87	3.14	---	71.60	20.94	3.09	---

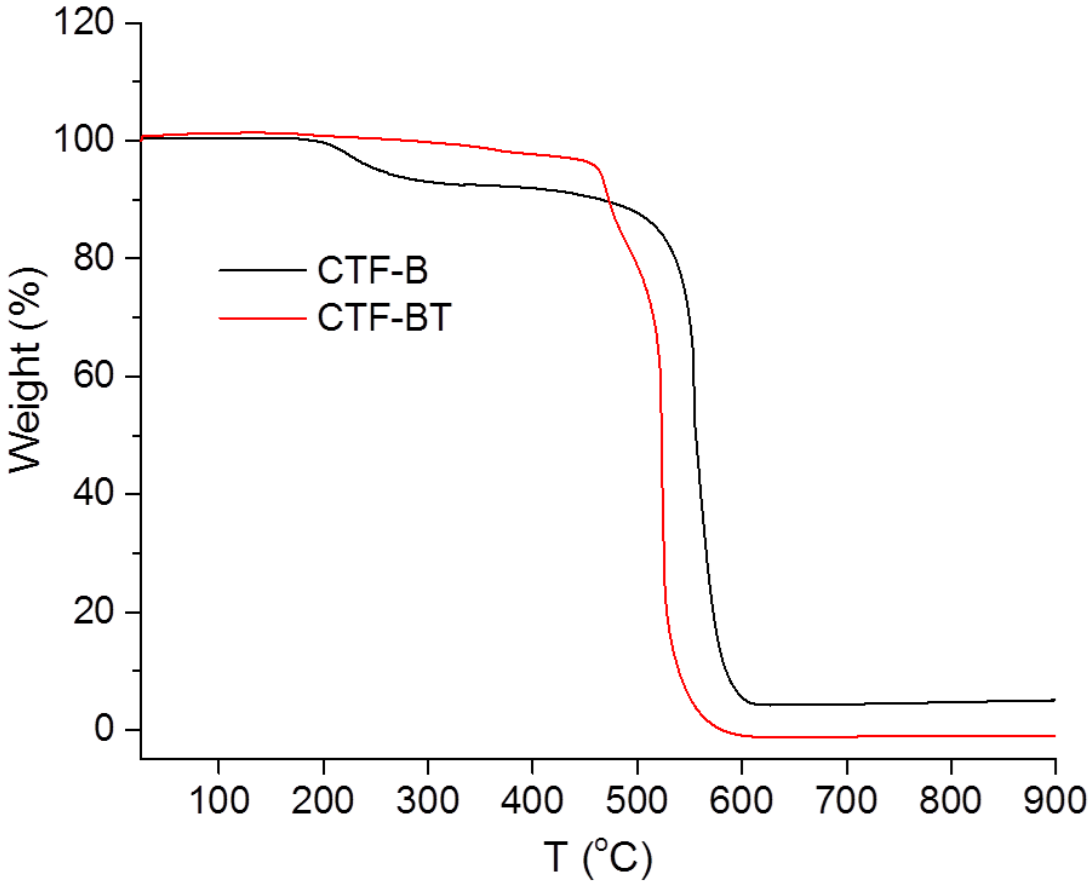

Fig. S11. TGA spectra of CTF-BT and CTF-B under O_2 atmosphere with a heating rate of 10 ^{o}C/min.

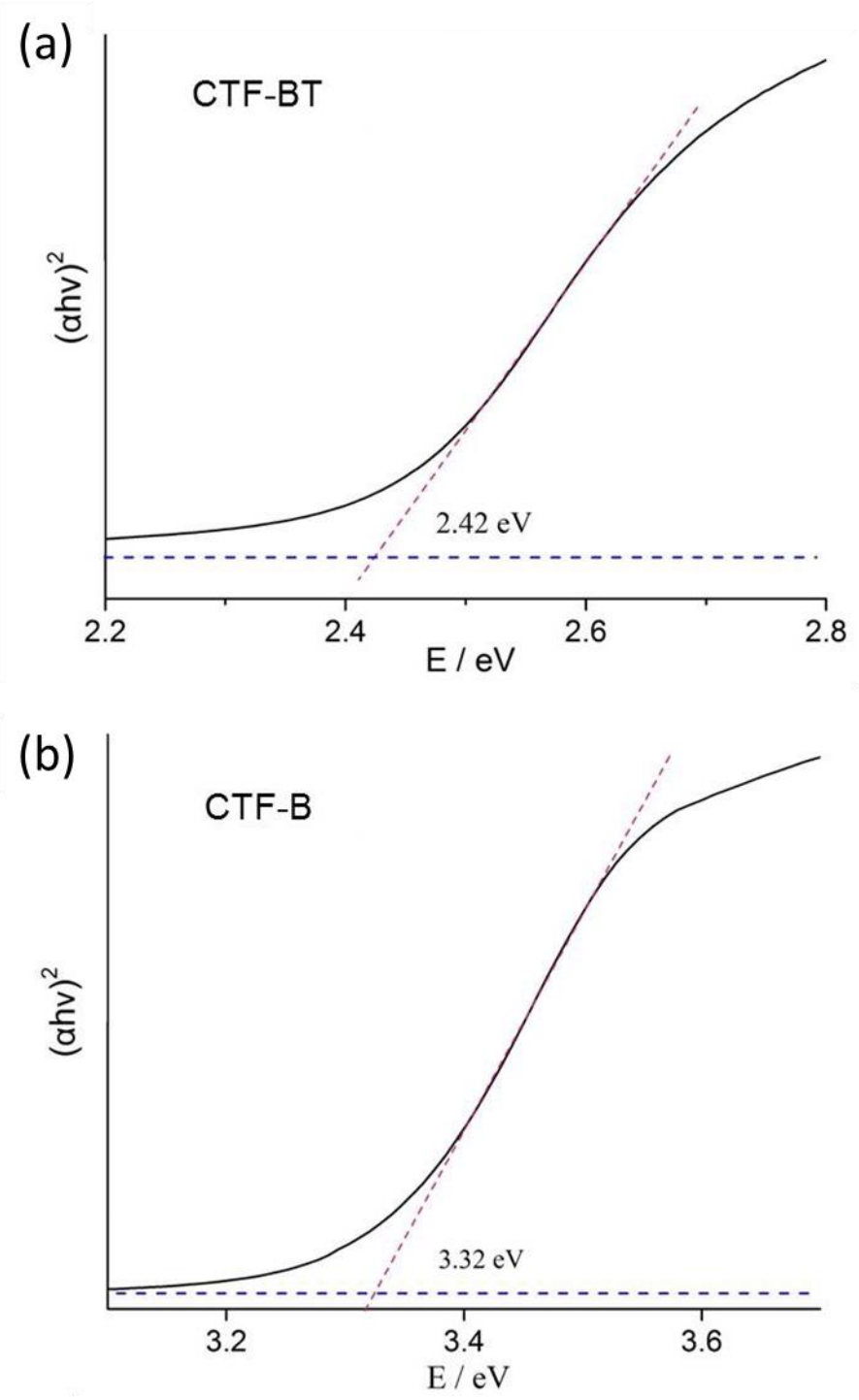

Fig. S12. Kubelka-Munk-transformed reflectance spectra of (a) CTF-B and (b) CTF-BT.

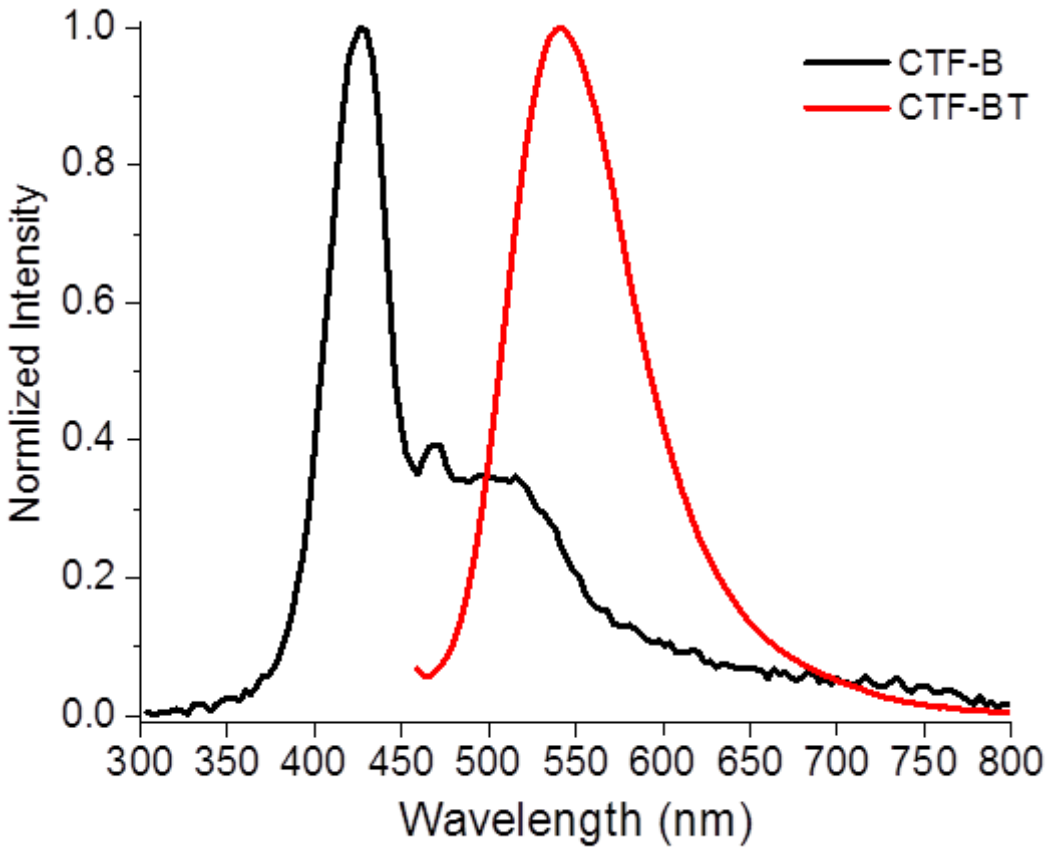

Fig. S13. Photoluminescence spectra of CTF-BT and CTF-B.

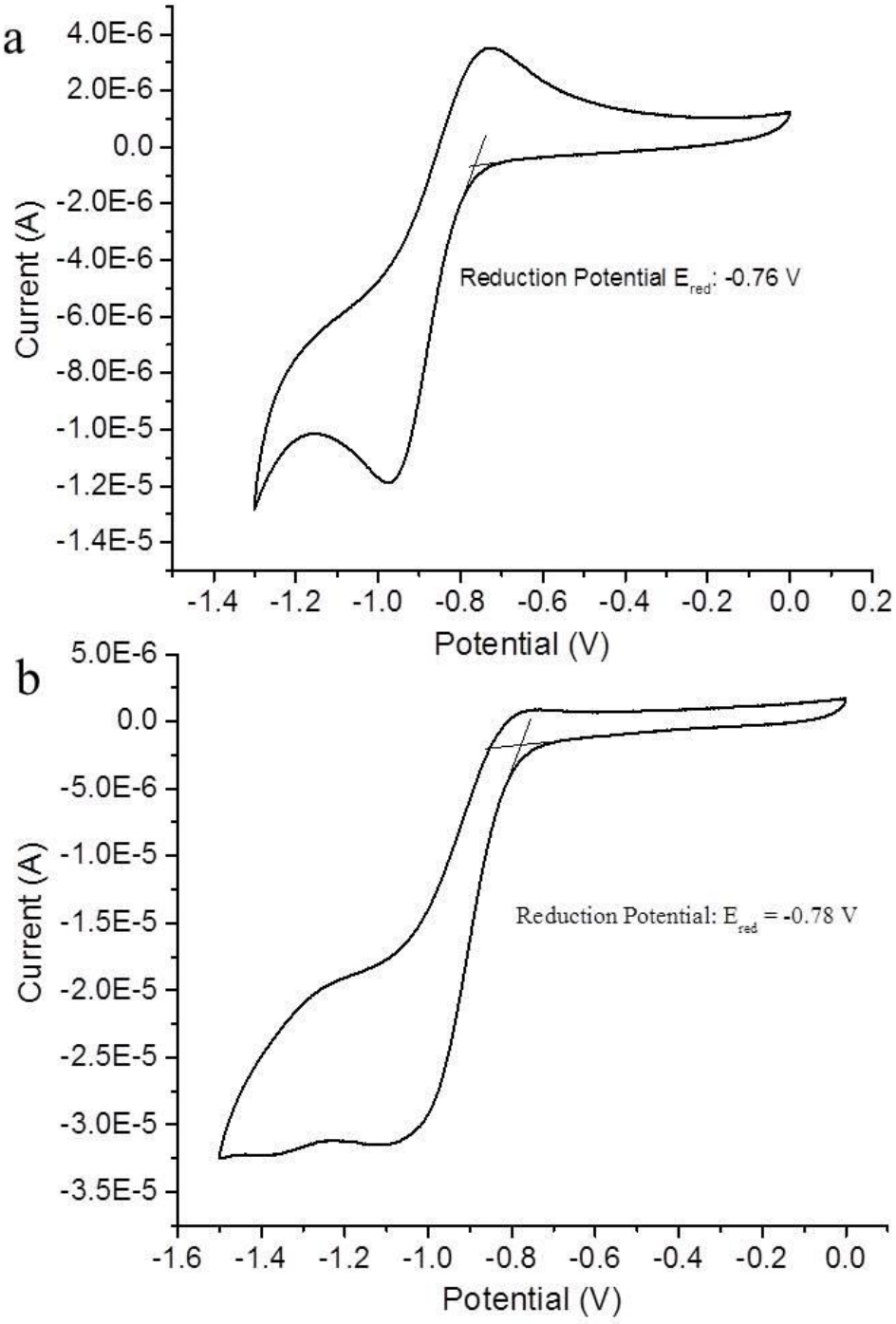

Fig. S14. Cyclic voltammetry measurements of a) nanoporous CTF-B and b) CTF-BT.

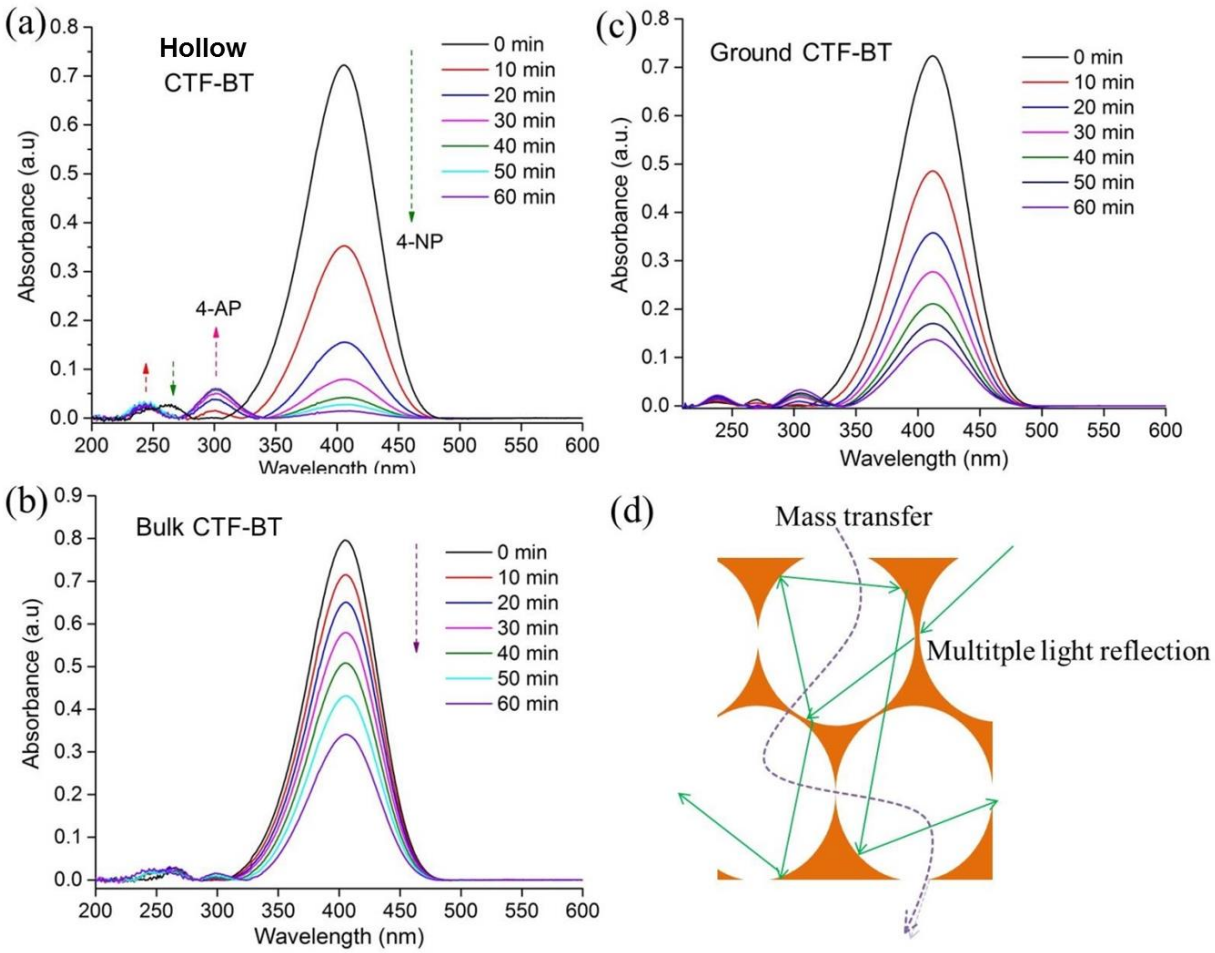

Fig. S15. UV-Vis spectra of 4-NP obtained at different time intervals using a) hollow CTF-BT, b) bulk CTF-BT and c) ground CTF-BT as photocatalyst, respectively. (d) Schematic illustration of enhanced mass transfer and multiple light reflections.

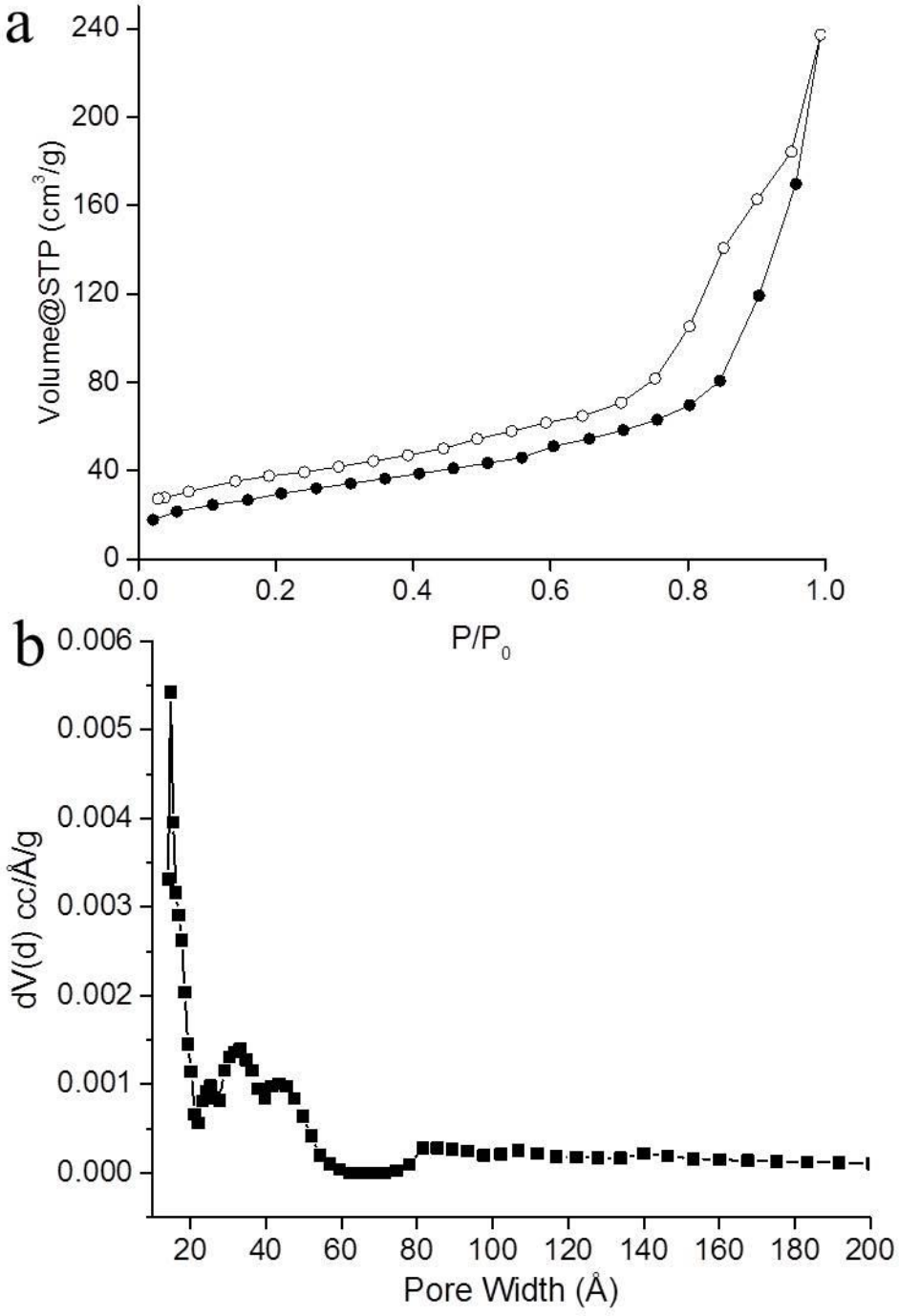

Fig. S16. N_2 gas absorption-desorption isotherm of the ground CTF-BT measured at 77 K and (b) pore size distribution.

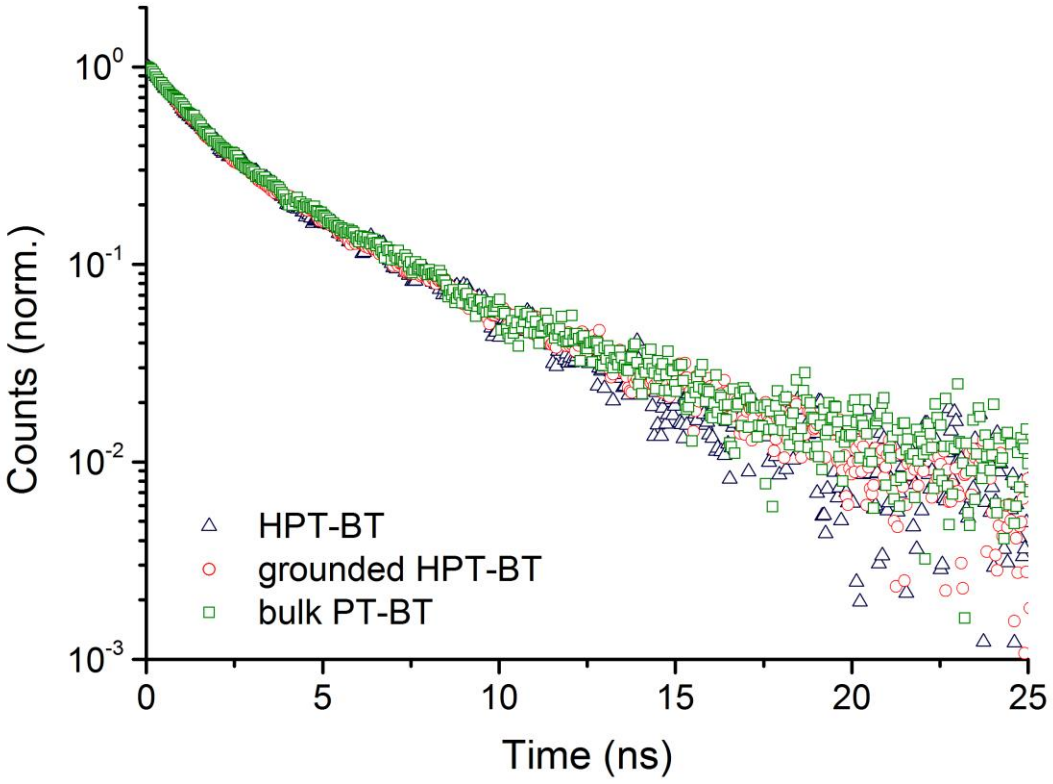

Fig. S17. Fluorescence decay monitored at 540 nm under excitation at 450 nm.

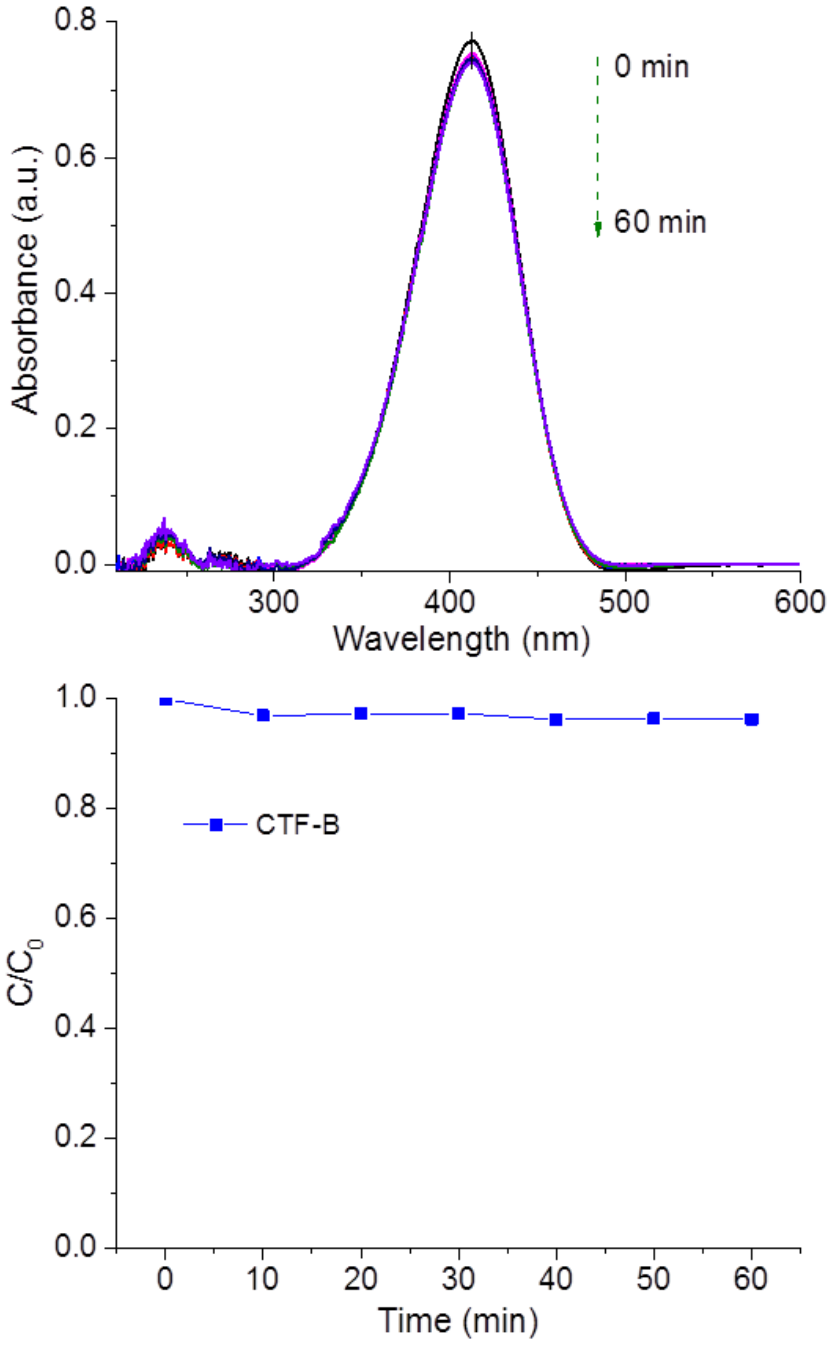

Fig. S18. UV-Vis spectra and photoreduction rates of 4-NP to 4-AP using CTF-B as photocatalyst.

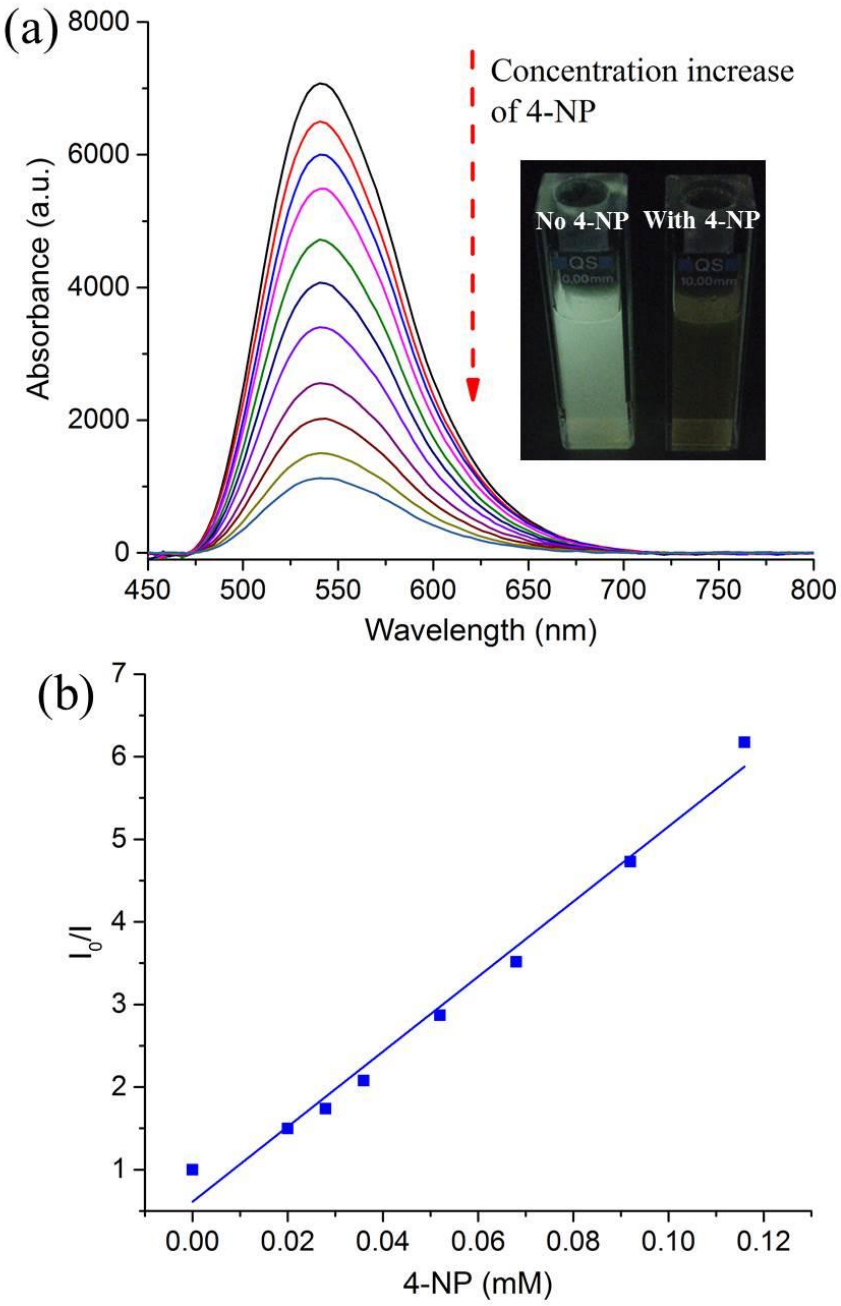

Fig. S19. (a) UV-Vis absorption spectra of CTF-BT in H_2O/EtOH (3:1) with increasing the concentration of 4-NP and (b) the corresponding emission intensity change curve.

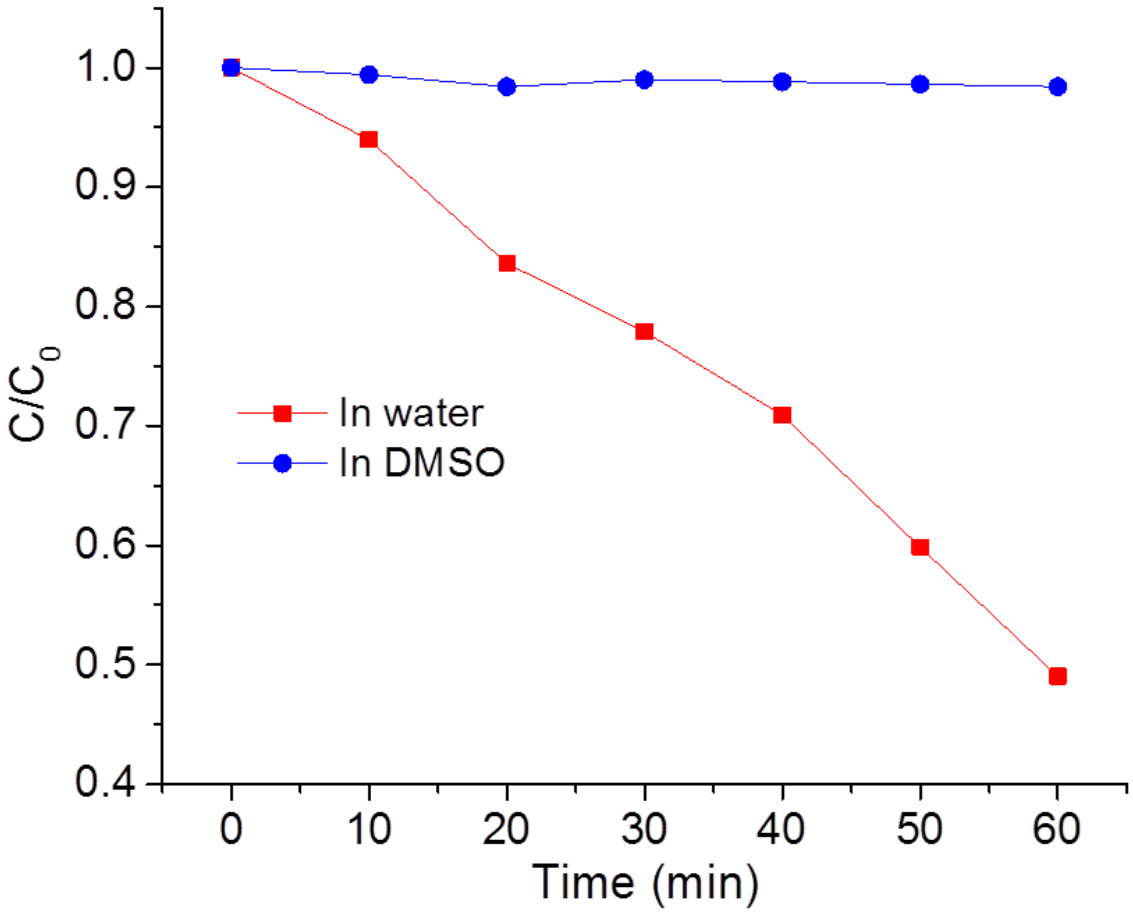

Fig. S20. Plot of C/C_0 versus irradiation time for the photoreduction of 4-NP using NaTPB as electron donor in water and in DMSO.

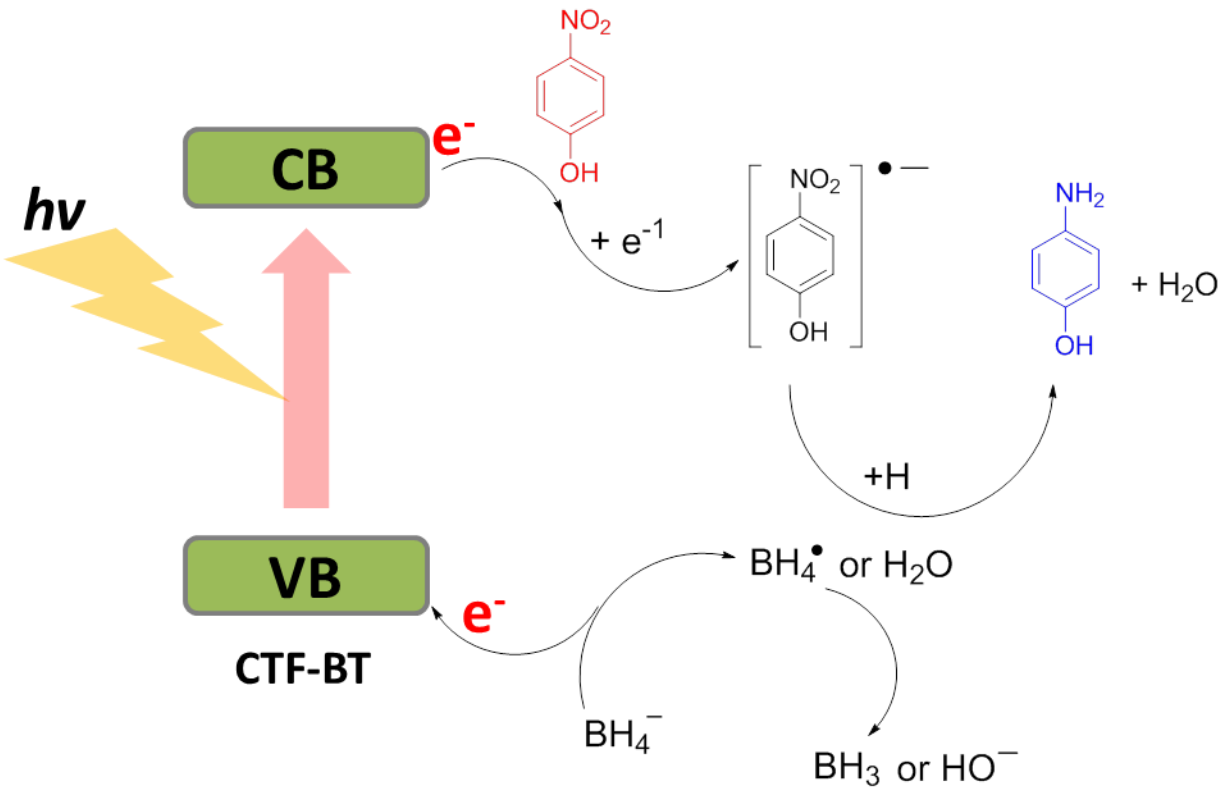

Fig. S21. Schematic mechanism of photocatalytic reduction of 4-NP to 4-AP.

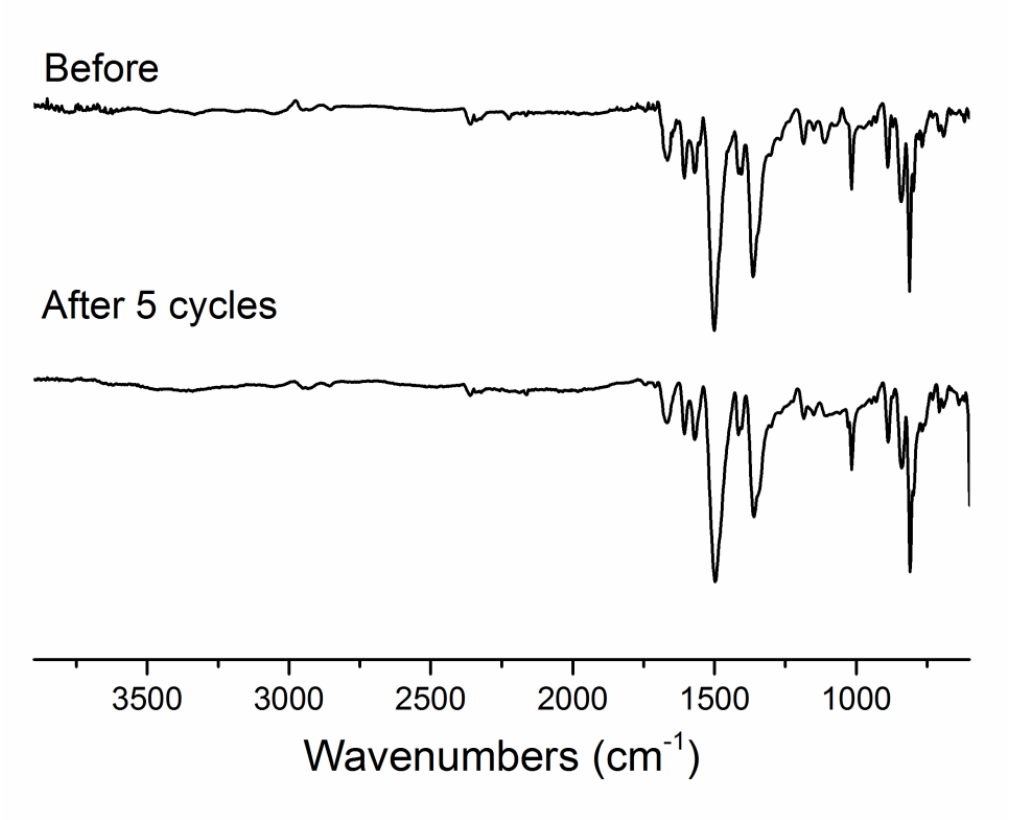

Fig. S22. FT-IR spectra of CTF-BT before and after five reaction cycles

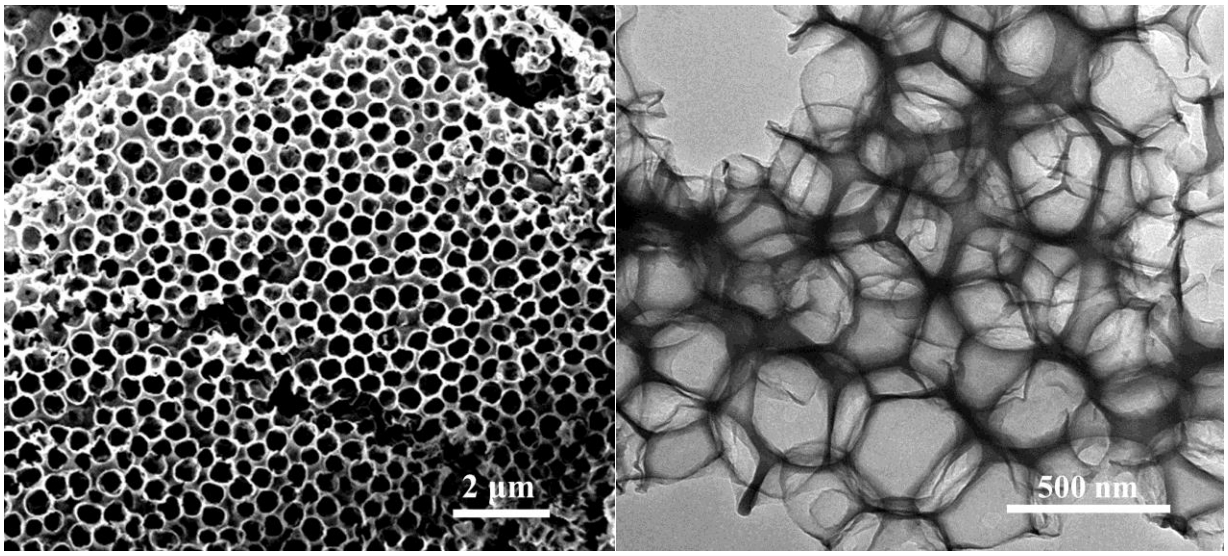

Fig. S23. SEM and TEM images of CTF-BT after five reaction cycles.

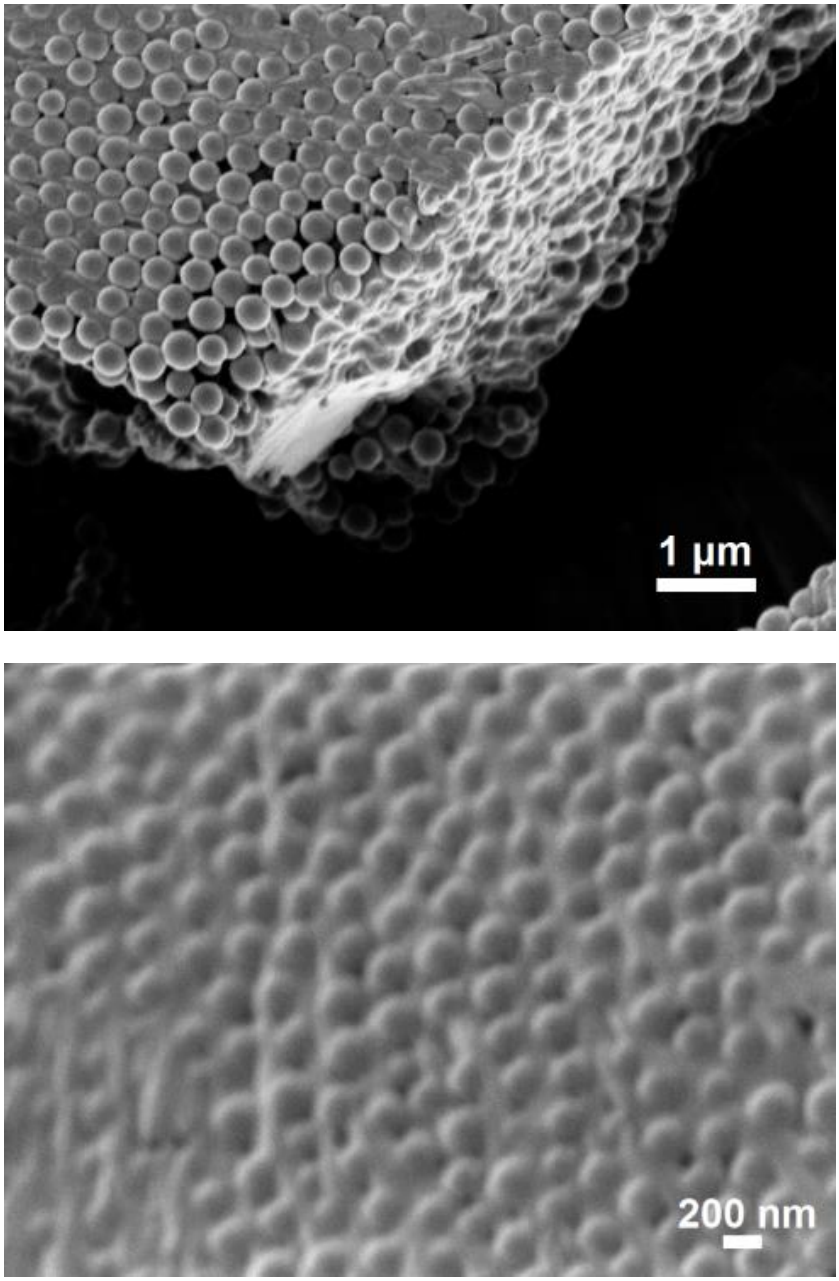

Fig. S24. Additional SEM images of initial BT-Ph_2-CN_2/silica nanoparticle precursor for CTF-BT.

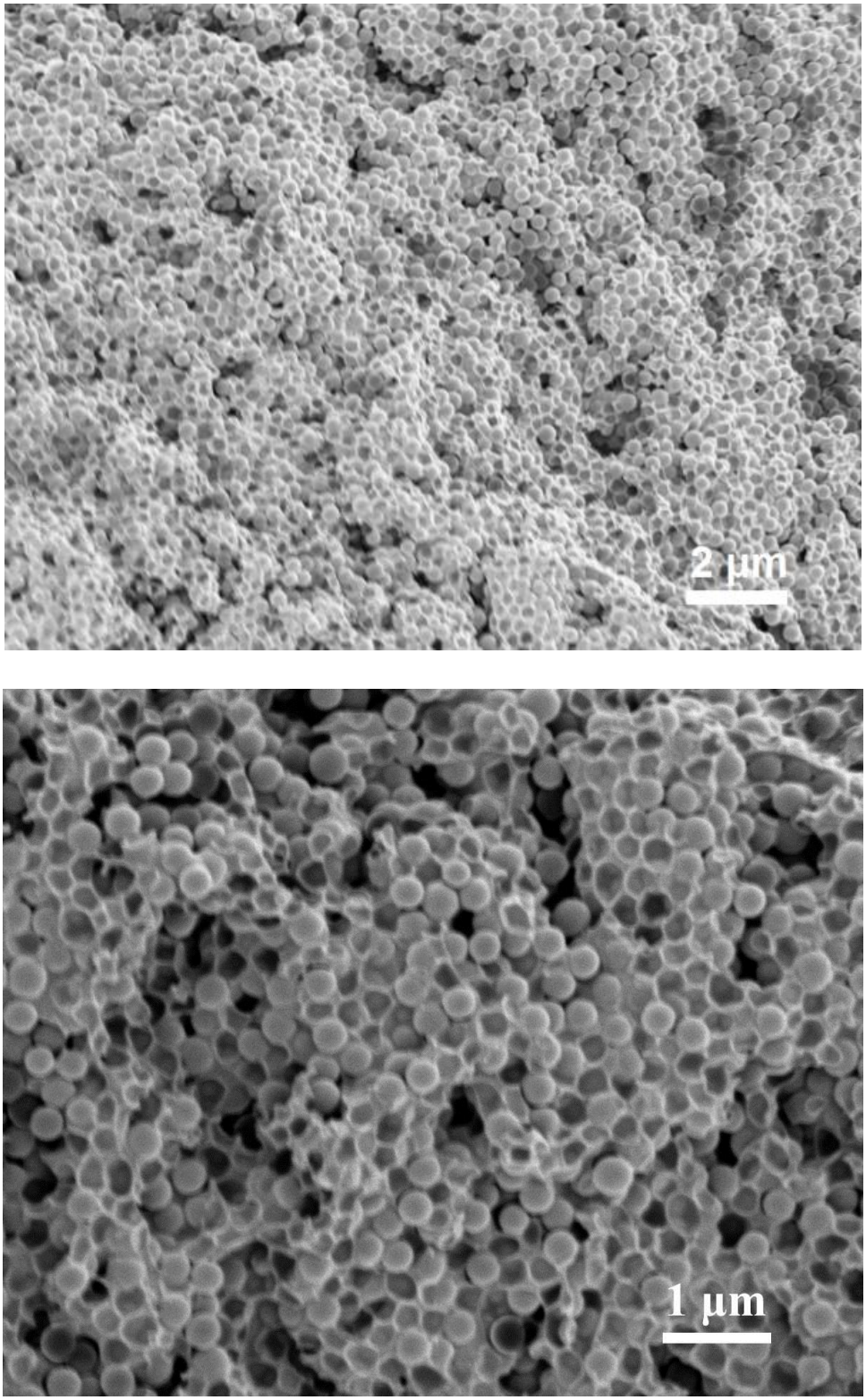

Fig. S25. SEM images of CTF-BT before silica removing

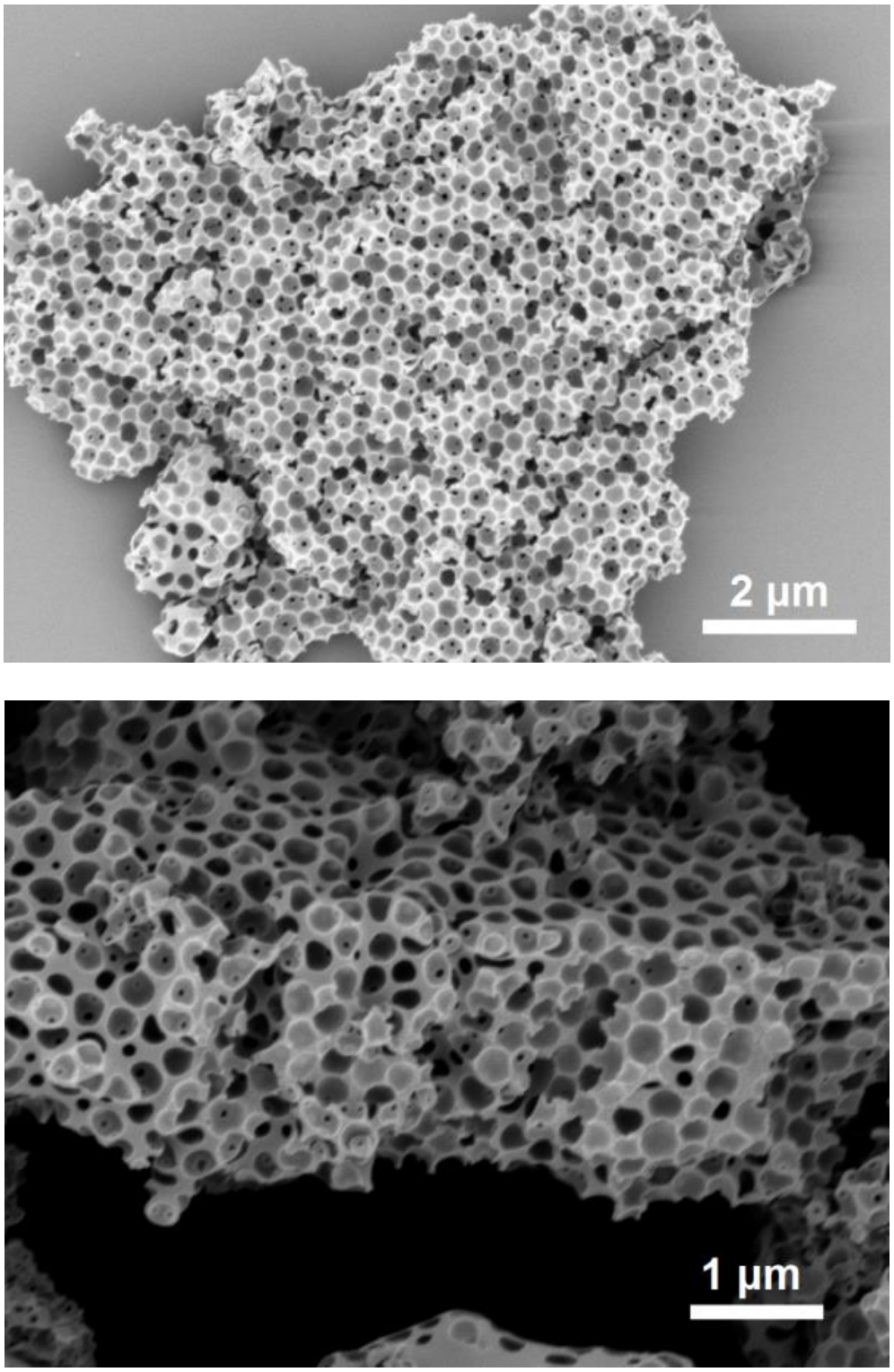

Fig. S26. Additional SEM images of hollow CTF-B.

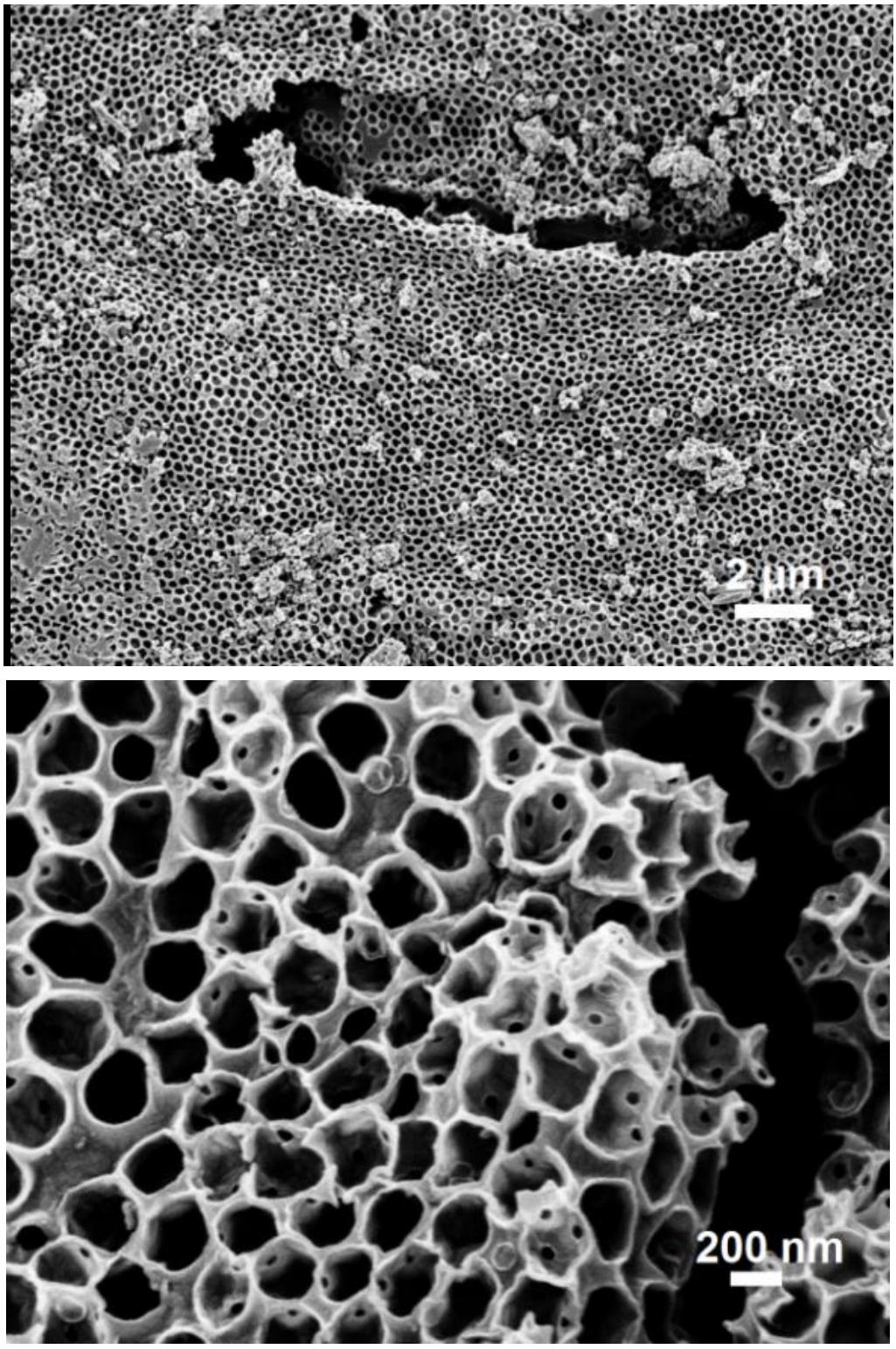

Fig. S27. Additional SEM images of hollow CTF-BT.

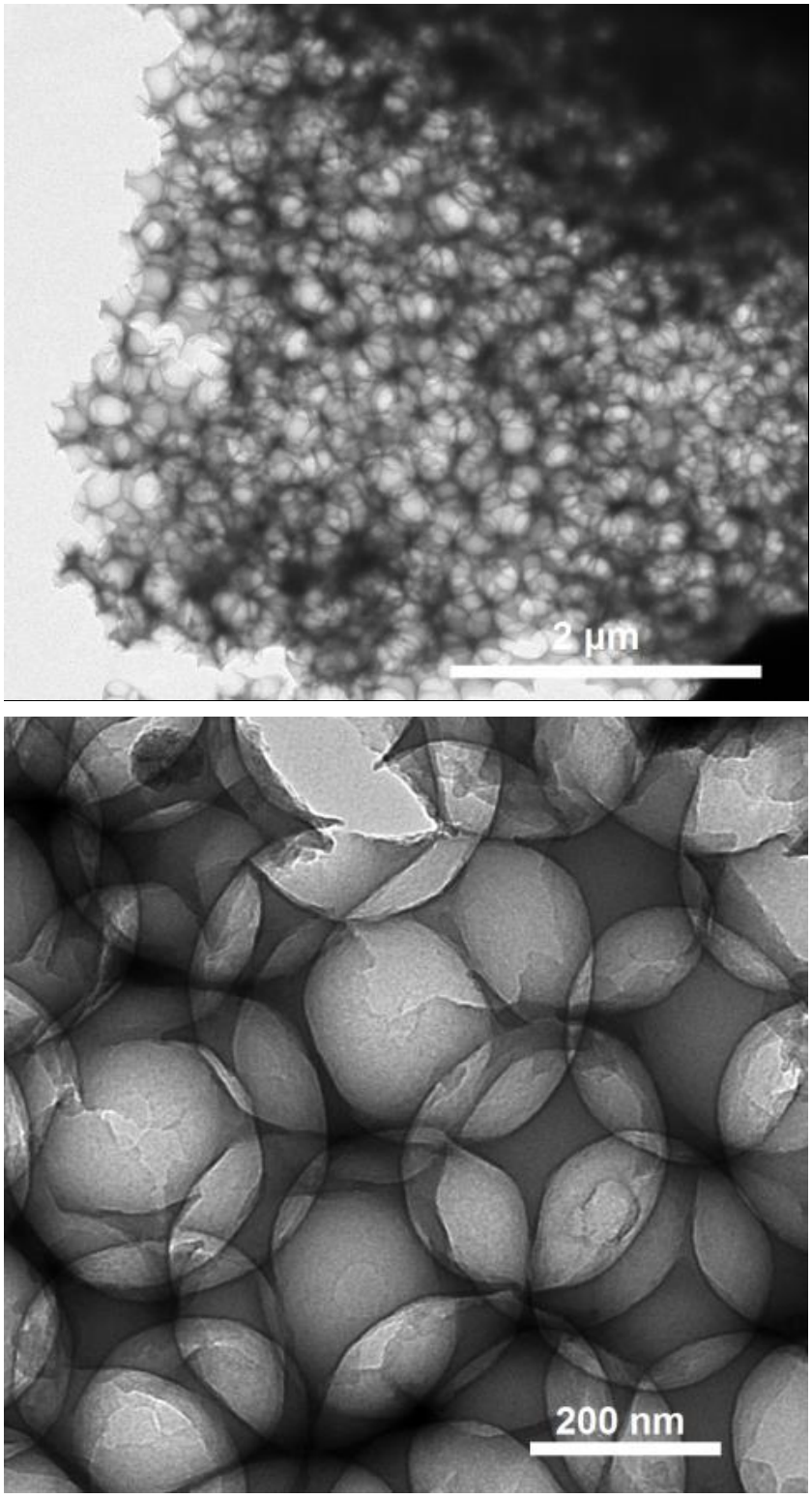

Fig. S28. Additional TEM images of hollow CTF-B.

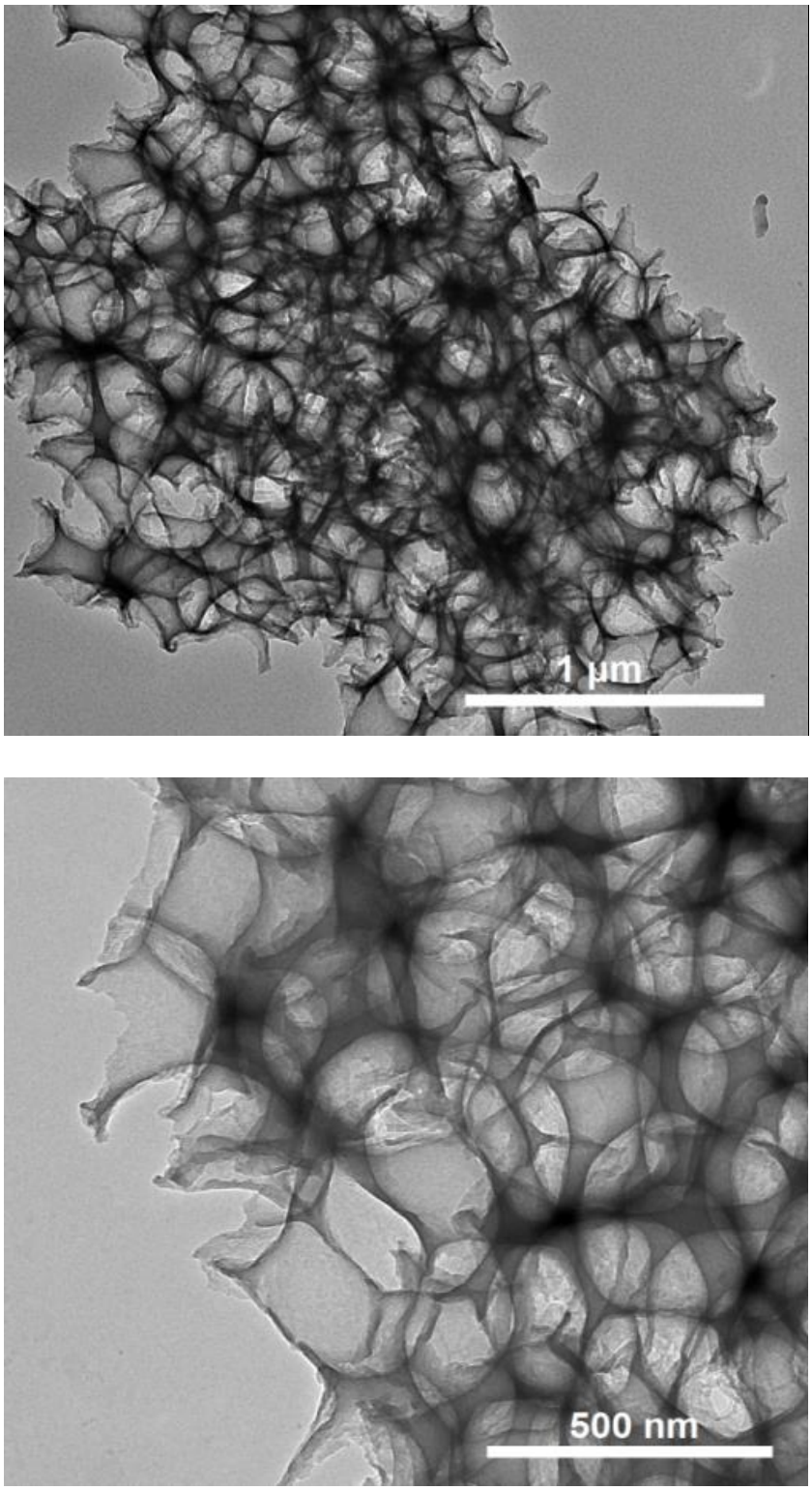

Fig. S29. Additional TEM images of hollow CTF-BT.

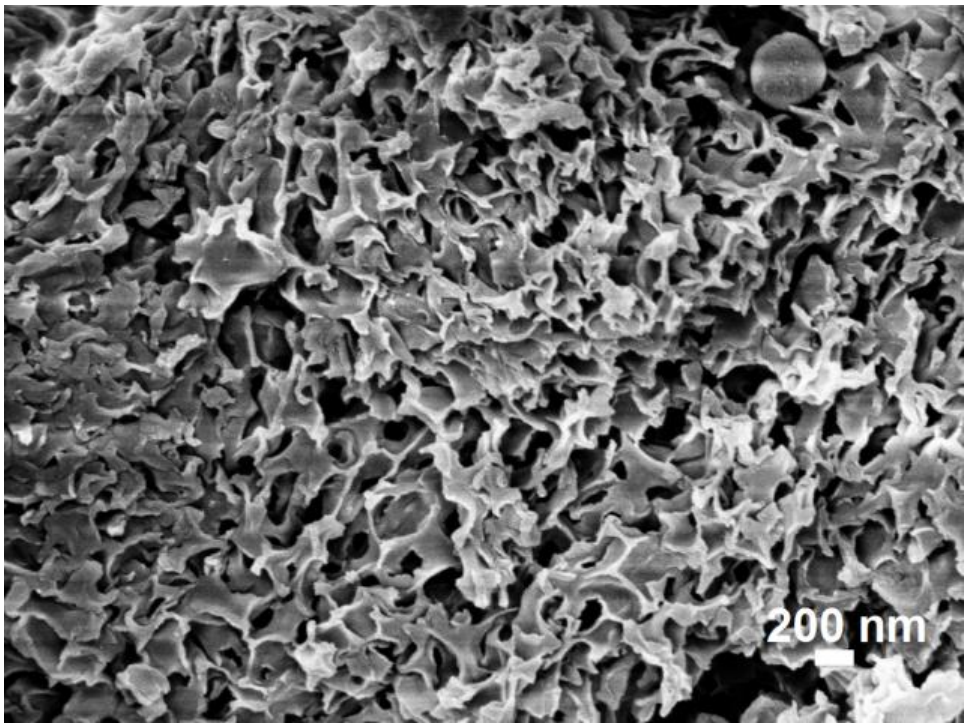

Fig. S30. SEM images of ground CTF-BT.

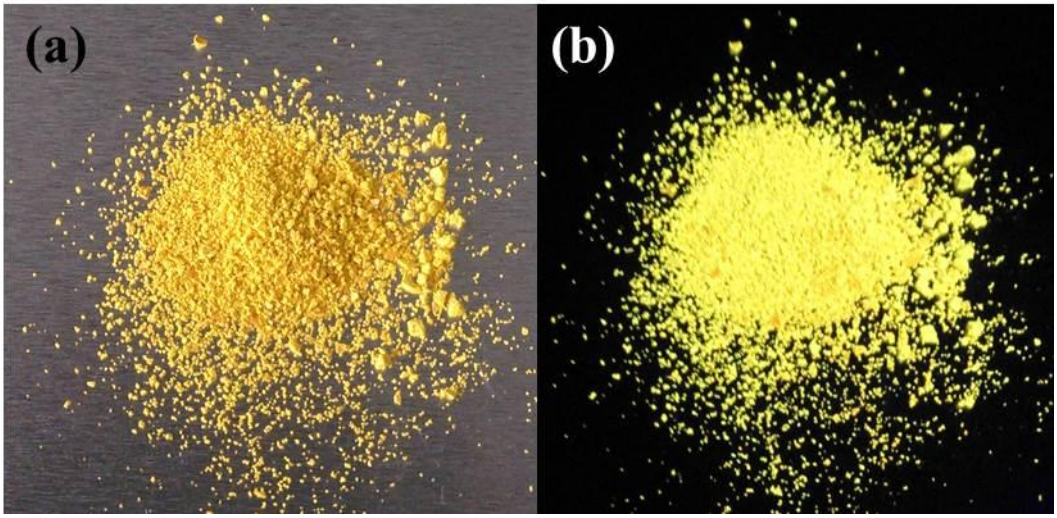

Fig. S31. Photograph of hollow CTF-BT (a) before and (b) after excitation under UV light (365 nm).

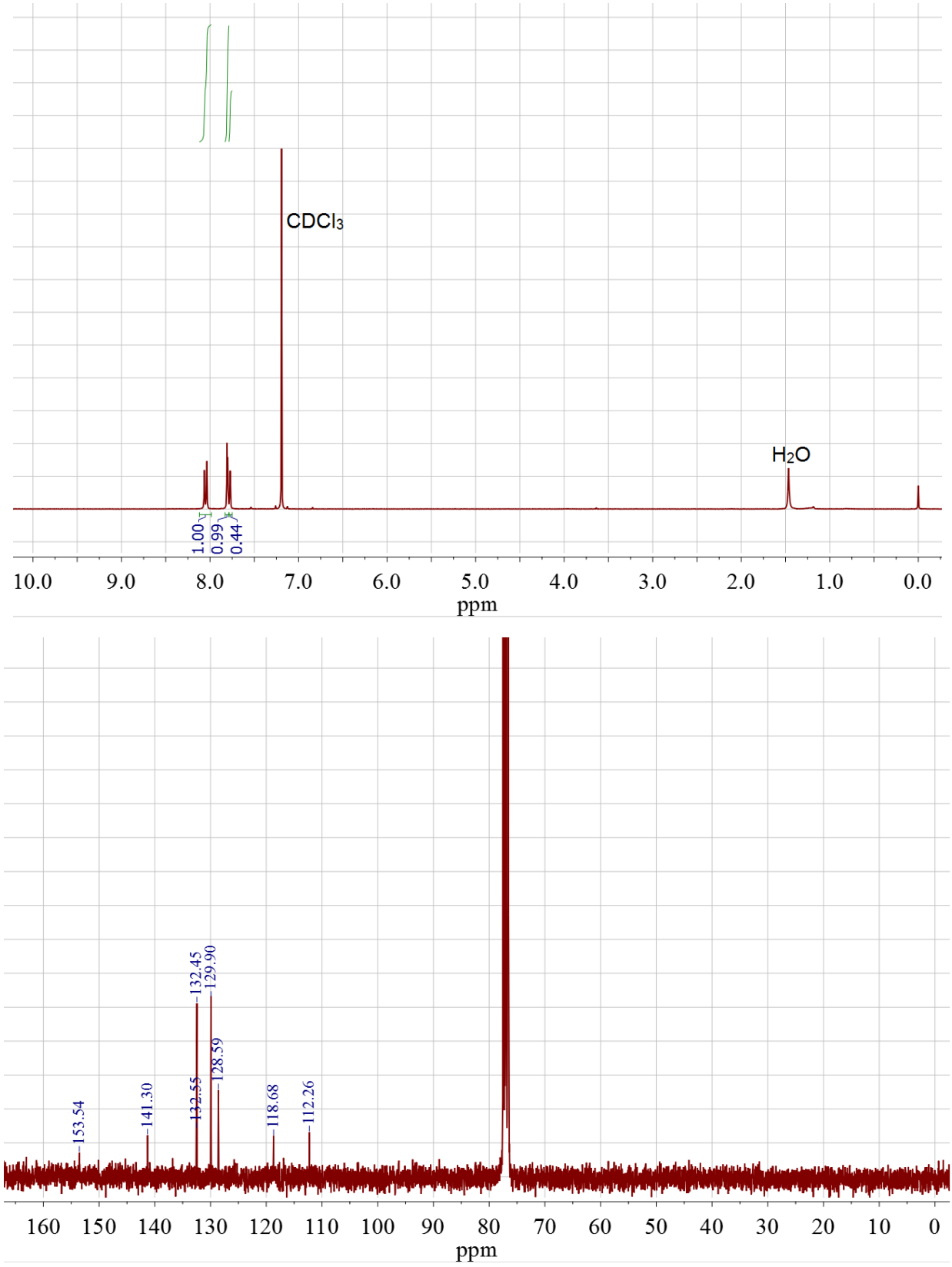

Fig. S32. ^{1}H NMR and ^{13}C NMR spectra of BT- Ph_2-CN_2 in $CDCl_3$.

[1] W. Stöber, A. Fink, E. Bohn, *Journal of colloid and interface science* **1968**, *26*, 62-69.